RESEARCH ARTICLE OPEN ACCESS

Gut Microbiota-Derived Extracellular Vesicles Influence Alcohol Intake Preferences in Rats

Macarena Díaz-Ubilla[1] | Aliosha I. Figueroa-Valdés[2] | Hugo E. Tobar[2] | María Elena Quintanilla[3,4,5] | Eugenio Díaz[3] | Paola Morales[3,4,5] | Pablo Berríos-Cárcamo[1] | Daniela Santapau[1] | Javiera Gallardo[1] | Cristian de Gregorio[1] | Juan Ugalde[6] | Carolina Rojas[7,8] | Antonia Gonzalez-Madrid[1] | Marcelo Ezquer[1] | Yedy Israel[3,5] | Francisca Alcayaga-Miranda[2,7] | Fernando Ezquer[1,9]

[1]Center for Regenerative Medicine, Faculty of Medicine, Clínica Alemana-Universidad del Desarrollo, Santiago, Chile | [2]Center of Interventional Medicine for Precision and Advanced Cellular Therapy (IMPACT), Santiago, Chile | [3]Molecular and Clinical Pharmacology Program, Institute of Biomedical Science, Faculty of Medicine, Universidad de Chile, Santiago, Chile | [4]Department of Neuroscience, Faculty of Medicine, Universidad de Chile, Santiago, Chile | [5]Specialized Center for Prevention of Substance Use and Treatment of Addictions (CESA), Faculty of Medicine, Universidad de Chile, Santiago, Chile | [6]Center for Bioinformatics and Integrative Biology, Facultad de Ciencias de la Vida, Universidad Andrés Bello, Santiago, Chile | [7]Centro de Investigación e Innovación Biomédica (CIIB), Facultad de Medicina, Universidad de Los Andes, Santiago, Chile | [8]Faculty of Dentistry, Universidad de Los Andes, Santiago, Chile | [9]Research Center for the Development of Novel Therapeutic Alternatives for Alcohol Use Disorders, Santiago, Chile

Correspondence: Fernando Ezquer (eezquer@udd.cl) | Francisca Alcayaga-Miranda (falcayaga@uandes.cl)

ABSTRACT

Growing preclinical and clinical evidence suggests a link between gut microbiota dysbiosis and problematic alcohol consumption. Extracellular vesicles (EVs) are key mediators involved in bacteria-to-host communication. However, their potential role in mediating addictive behaviour remains unexplored. This study investigates the role of gut microbiota-derived bacterial extracellular vesicles (bEVs) in driving high alcohol consumption. bEVs were isolated from the gut microbiota of a high alcohol-drinking rat strain (UChB rats), either ethanol-naïve or following chronic alcohol consumption and administered intraperitoneally or orally to alcohol-rejecting male and female Wistar rats. Both types of UChB-derived bEVs increased Wistar's voluntary alcohol consumption (three bottle choice test) up to 10-fold ($p < 0.0001$), indicating that bEVs are able and sufficient to transmit drinking behaviour across different rat strains. Molecular analysis revealed that bEVs administration did not induce systemic or brain inflammation in the recipient animals, suggesting that the increased alcohol intake triggered by UChB-derived bEVs operates through an inflammation-independent mechanism. Furthermore, we demonstrate that the vagus nerve mediates the bEV-induced increase in alcohol consumption, as bilateral vagotomy completely abolished the high drinking behaviour induced by both intraperitoneally injected and orally administered bEVs. Thus, this study identifies bEVs as a novel mechanism underlying gut microbiota-induced high alcohol intake in a vagus nerve-dependent manner.

1 | Introduction

Problematic alcohol consumption is a major public health concern and a significant risk factor for the development of hundreds of diseases (Alcohol 2008). Alcohol use disorder (AUD) is also associated with significant social and familial problems; it has been reported that first-degree relatives of individuals with AUD are two to seven times more likely to develop alcohol dependence during their lifetime than people with non-alcoholic relatives (Berent and Wojnar 2021). One typically overlooked trait shared between family members is the microbiota, which refers to the living microorganisms inhabiting a defined environment, such as the gut (Hou et al. 2022). Each family possesses such a distinctive microbiota composition that it allows the identification of single families within a cohort of individuals from the same geographic region (Schloss et al. 2014; Song et al. 2013; Valles-Colomer et al. 2023). Shared diets, genes and general lifestyle shape the family's microbiota compositions, starting when mothers transmit their microbiota to their offspring (Ferretti et al. 2018; Tian et al. 2023); this inherited microbiota is referred to as innate microbiota.

Alterations in gut microbiota composition have been clearly correlated with increased consumption of drugs of abuse, including morphine (Lee et al. 2018), cocaine (Kiraly et al. 2016; Tran et al. 2023) and alcohol (Ezquer et al. 2022; Ezquer et al. 2021; Reyes et al. 2020). In our previous research with the UChB rat strain, which are Wistar-derived rats selected and bred for several generations based on their high alcohol preference (Israel et al. 2017; Quintanilla et al. 2006), a specific innate gut microbiota composition was identified as a key heritable trait predisposing these animals to high voluntary alcohol intake (Ezquer et al. 2022; Ezquer et al. 2021). Interestingly, oral administration of non-absorbable antibiotic treatment to disrupt the innate gut microbiota composition in UChB rats resulted in a remarkable 70% inhibition in voluntary ethanol consumption compared to vehicle-treated animals. 16S rRNA sequencing analysis of faeces collected before and after treatment revealed antibiotics reduced the relative abundance of Proteobacteria and increased the relative abundance of Bacteroidetes at phylum level (Ezquer et al. 2021). Interestingly, in studies of patients with a drinking history, the relative abundance of the phylum Proteobacteria was increased and Bacteroidetes was decreased (Chen et al. 2022), suggesting that common microbiota components between UChB rats and humans could be pointed out as protective or permissive, regarding alcohol consumption. Likewise, recent studies have also reported the promotion of high alcohol consumption in mice following a gut microbiota transplant from patients with AUD, confirming the pivotal role of gut microbiota in influencing alcohol-related behaviours (Bajaj et al. 2021; Wolstenholme et al. 2022; Zhao et al. 2020). Collectively, these findings support the notion of alcoholism as a modifiable and potentially transmissible behaviour, mediated by the intricate interplay of gut microbiota, even across different species.

Several bidirectional gut microbiota–brain communication pathways have been established, encompassing endocrine, immune, and neural pathways (Cryan and Dinan 2012). Regarding alcohol dependence, both systemic and brain inflammation, mainly mediated by the activation of glial cells in the prefrontal cortex (PFC) and nucleus accumbens (NAc), have emerged as one of the main addiction-related or triggering processes (Blednov et al. 2011; Everitt and Robbins 2005; Koob and Volkow 2016; Ostlund and Balleine 2005). Astrocyte activation in the PFC appears to be required to trigger a drinking behaviour in ethanol-naïve mice (Erickson et al. 2021). Microglia, likewise, plays a significant role in alcohol intake since mice treated with minocycline—an antibiotic known to suppress microglia activation—significantly reduced their voluntary ethanol intake (Agrawal et al. 2011). Recent evidence suggests that gut microbiota is an important source of inflammation that can modulate behaviour (Leclercq et al. 2017; Xie et al. 2023). One element that could be mediating microbiota-induced inflammation are extracellular vesicles (EVs), as these nanovesicles are well-established key players in interkingdom communication, including interactions between microbial and mammalian host cells (Castano et al. 2023; Schuh et al. 2019).

Gut microbiota-derived EVs are highly heterogeneous, encompassing a broad spectrum of EVs originating from bacteria, fungi and protozoa. Among these EVs, bacterial EVs (bEVs) have gained significant attention, given the predominant presence of bacteria cell numbers within the gut milieu compared to other microorganisms (Haas-Neill and Forsythe 2020).

bEVs are lipid bilayer vesicles ranging in size from 20 to 400 nm that are constantly produced and released by pathogenic and commensal Gram-negative (called outer membrane vesicles; OMVs) and Gram-positive (called membrane vesicles; MVs) bacteria (Haas-Neill and Forsythe 2020). Although these bEVs are generated through different biogenesis processes, both bEVs types can mediate cell-to-cell communication by delivering DNA, RNA, proteins, lipids and other specific metabolites (Berleman and Auer 2013; Haas-Neill and Forsythe 2020). Notably, circulating gut-derived bEVs have been detected in the bloodstream of mice, characterised by the presence of lipopolysaccharide (LPS) (bEVs derived from Gram-negative bacteria) and lipoteichoic acid (LTA) (bEVs derived from Gram-positive bacteria) (Ou et al. 2023). bEVs have also been identified in healthy donors' human red blood cell concentrates, whose characterisation determined the presence of LPS and outer membrane protein A (OmpA) (Schaack et al. 2022). The presence of OmpA marker, specific for the *Enterobacteriaceae* family, suggests that the origin of these bEVs is the gut microbiota (Schaack et al. 2022). Due to their nano size and membranous nature, bEVs are capable of transporting molecules between distant organs, including those conforming to the gut-brain axis. In vivo studies in murine models have reported the ability of bEVs to cross the blood–brain-barrier (BBB), triggering neuroinflammation, neuronal damage, and alterations in glial function (Palacios et al. 2023; Wei et al. 2020). Interestingly, the effect of gut microbiota and gut microbiota-derived bEVs upon brain function and behaviour relies not only on the vesicles entering the systemic circulation but also locally on the vagus nerve (Lee et al. 2020). The vagus nerve has both efferent and afferent fibres, with approximately 80% of them being sensory, conveying information about the state of the body's organs to the central nervous system (CNS) (Howland 2014). It has been previously reported that UChB rats reduced their high voluntary alcohol intake by 75% after a bilateral vagotomy was performed (Ezquer et al. 2021). In the same sense, vagotomy not only prevented the reduction in anxiety and despair-like

behaviour resulting from the oral administration of *L. rhamnosus* (JB-1) in mice (Bravo et al. 2011), but it also significantly alleviated cognitive impairment and reduced bacterial 16S rDNA levels detected in the hippocampus of mice treated with *P. hominis* bEVs delivered by oral gavage (Lee et al. 2020).

To our knowledge, no evidence has yet been shown to establish a link between gut microbiota-derived bEVs and drug addiction, nor has it been demonstrated that these bEVs are sufficient to transmit addictive behaviour. Therefore, this study aims to evaluate whether gut microbiota bEVs derived from the high alcohol drinking UChB rat strain can promote drinking behaviour in alcohol-rejecting Wistar rats and to investigate the effects of the bEVs administration on systemic and brain inflammation. Additionally, we evaluated the role of the vagus nerve in mediating the increase in voluntary alcohol consumption after the bEVs administration as modified by a bilateral vagotomy.

2 | Methods

2.1 | Gut Microbiome Analysis

Two-months-old male UChB rats—Wistar-derived rats selectively bred for over 90 generations as alcohol consumers—(Israel et al. 2017; Quintanilla et al. 2006) and 2-months-old male Wistar rats were used for gut microbiota isolation. Animals were housed individually in acrylic cages, maintained on a 12-h light/dark cycle, and regularly fed a soy protein, peanut-meal rodent diet (Cisternas, Santiago, Chile). Experimental procedures were approved by the Ethics Committee for Experiments with Laboratory Animals from the Faculty of Medicine, Universidad de Chile (Protocol CBA 0994 FMUCH).

UChB animals were randomly assigned into two groups (six animals per group), and one group received continuous free-choice access to 10% (v/v) ethanol solution and water concurrently for 120 days (UChB-Alcohol group), while the other group had access to water only (UChB-Water group). The ethanol intake of the alcohol-consuming group ranged between 10 and 12 g ethanol/kg/day. Additionally, a group of six male Wistar animals exposed to water only for the same 120-day period served as a control (Wistar group).

For analysis of gut microbiota composition, fresh stool samples were individually collected from the three experimental groups and immediately stored at −80°C until use. Genomic DNA was purified using the Presto Mini gDNA Bacteria Kit (Geneaid Biotech Ltd.; Cat. #GBB100) following the manufacturer's instructions.

Briefly, 200 mg of frozen stool material per individual were minced and suspended by vortexing in nuclease-free water. After a single spin, the supernatant was recovered and centrifuged for 1 min at $16,000 \times g$. The pellet was resuspended in 200 µL of G+ buffer with Lysozyme and incubated at 37°C for 30 min. Next, 180 µL of GT Buffer were added to the sample and vortexed, followed by the addition of 20 µL of Proteinase K. The mixture was incubated at 60°C for 10 min. Lysis was achieved by adding 200 µL of GB Buffer, vortexing for 10 s, and incubating at 70°C for 10 min. For DNA binding, 200 µL of absolute ethanol were added to the sample lysate and mixed by shaking. The mixture was then transferred to a GD column and centrifuged at $16,000 \times g$ for 2 min. The column was washed with 400 µL of W1 Buffer and centrifuged at $16,000 \times g$ for 30 s, followed by a second wash with 600 µL of Wash Buffer, and centrifuged again at $16,000 \times g$ for 30 s. The column was dried by centrifuging at $16,000 \times g$ for 3 min. DNA was eluted with 100 µL of Elution Buffer by centrifugation at $16,000 \times g$ for 30 s. The purified DNA was quantified using a Qubit 4 Fluorometer with the dsDNA HS Assay Kit (Invitrogen; Cat. #Q32851).

DNA sequencing was performed by Macrogen (Korea) by creating multiplexed barcoded amplicons for 16S rRNA V3-V4 regions. Data was processed using nf-core/ampliseq version 2.11.0 (Straub et al. 2020), utilising software environments from the Bioconda (Gruning et al. 2018) and Biocontainers (da Veiga Leprevost et al. 2017) projects. Primer removal and sequence trimming was performed with Cutadapt, with default parameters. Amplicon sequence variants (ASV) were generated using DADA2 (Callahan et al. 2016), by first removing possible PhiX contamination, followed by trimming of the forward reads (283 bp) and reverse reads (222 bp). Chimera-free ASVs were taxonomically classified using DADA2 against the SBD-GTDB-Sativa curated 16S GTDB database (Release R09-RS220-1). Filtering of the ASVs was performed using Phyloseq, where all ASVs that were part of a Phylum with a mean prevalence of less than 1 and a total read abundance of less than 100 were filtered. Then, any ASV with no taxonomic classification at the Phylum level were removed as well. Visualisation and statistical analysis were performed in R, using the Phyloseq (McMurdie and Holmes 2013), microViz (Barnett et al. 2021), ampvis2 and ggstatsplot packages (Patil 2021).

Statistical modelling of taxa between different sample groups was performed using microViz (Barnett 2021), by grouping all ASVs at the genus level, followed by a compositional normalisation. A minimum prevalence of 10% was considered, and the data was log2-transformed. The 16S rRNA sequencing data have been deposited in the Bioproject (NIH) database under the accession number PRJNA1195973, https://www.ncbi.nlm.nih.gov/bioproject/PRJNA1195973.

2.2 | Isolation of Gut Microbiota-Derived bEVs

For isolation of gut microbiota-derived bEVs, 5 g of fresh stool samples from animals of each experimental group (UChB-Alcohol, UChB-Water and Wistar group) were collected and immediately stored at −80°C until further processing for bEVs purification. To isolate gut microbiota-derived bEVs, stool samples were minced using a scalpel and then homogenised in 50 mL of 0.1 M phosphate buffer (PBS) pH 7.4 (Gibco, Cat. # 10010072) containing an EDTA-free protease inhibitor tablet (Roche, Complete, Cat. # 11836170001). After centrifugation at $8000 \times g$ for 15 min at 4°C, the supernatant (SN) was recovered and filtered with a 40 µm cell filter (Falcon, Cat. #352340). Subsequently, the SN was centrifuged at $10,000 \times g$ for 10 min at 4°C and again filtered with a 0.22 µm PES filter (Nest; Cat #331011). Then, the sample was subjected to an ultracentrifugation cycle at $100,000 \times g$ for 60 min at 4°C in an ultracentrifuge (Thermo Electron LED GmbH, model Sorvall WX+) using a swinging

bucket rotor (Thermo Fisher Scientific, Waltham, Model TH-641). The precipitated EVs were resuspended in 0.1 M PBS and then purified using a size exclusion chromatography (SEC) column (qEVsingle 70 nm isolation range, IZON, Cat # ICS70-1388) following the manufacturer's recommendations. Twelve fractions of 100 µL each were collected, and to identify the EV-enriched fraction, nanoparticle tracking analysis (NTA) (NanoSight NS300, Malvern Instruments Limited) was performed as described below. The first four fractions were selected because they contained particle enrichment in the size range expected for bEVs and were then pooled into a final volume of 400 µL. Amicon Ultra-15 10 KDa molecular weight cut-off filters (Merck, Cat # UFC901024) were used to concentrate the particle sample using centrifugation cycles of $4000 \times g$ for 10 min at 4°C until a final volume of 150 µL was obtained. Finally, the concentration of particles in the final concentrate was determined by NTA analysis. The isolated particles were stored at –80°C until use.

2.3 | bEVs Characterisation

The characterisation of bEVs in terms of size, concentration, morphology, integrity, presence of Gram-positive and Gram-negative markers and nucleic acid content was performed considering the MISEV2023 guidelines (Welsh et al. 2024), and following the protocols previously described in detail by our team (Figueroa-Valdes et al. 2021).

2.3.1 | Nanoparticle Tracking Analysis

The size and particle concentration were quantified by NTA using a NanoSight NS300 system (Malvern Instruments Ltd.). To avoid underestimation or overestimation, appropriate dilutions of the bEV samples were performed to obtain between 20 and 60 particles per frame. Five videos of 60 s each per sample were captured (camera level = 8; temperature control set to 25°C), processed (detection threshold = 3), and analysed to obtain the size mode and concentration of particles (software version: NTA 3.2 Dev Build 3.2.16; Malvern Instruments Ltd.).

2.3.2 | Endotoxin Quantification

LPS level was quantified in the isolated bEVs using the Endosafe-PTS LAL assay, an FDA-licensed endotoxin detection system (Charles River Laboratories, license #1197), using pre-filled cartridges (Charles River Laboratories; Cat #PTS20F) containing LAL reagent and chromogenic substrate. A 100 µL of 1:10,000 dilution of the bEV samples (total particles range: $1.4–5.0 \times 10^9$) was mixed with LAL reagent within the four-channel cartridge (25 µL per channel), two of which serve as endotoxin-spiked positive controls, following the manufacturer's instruction. The assay has a sensitivity of 0.05 EU/mL.

2.3.3 | Western Blot Analysis

To evaluate bacterial and eukaryotic protein markers, Western blots were performed following the protocols described by (Figueroa-Valdes et al. 2021) using Mini-PROTEAN Tetra Vertical Electrophoresis system (BIO-RAD, Cat #1658025FC) and Chameleon Duo pre-stained protein ladder (LI-COR, Cat #928-60000). Proteins were transferred to a 0.45 µm pore size PVDF membrane (Thermo Scientific, Cat #88518) by Mini Trans-Blot wet/tank blotting system (BIO-RAD, Cat #1658030). For bEVs, 40 µL of isolated bEV samples derived from Wistar, water- and alcohol-consuming UChB rats were loaded per lane. The detection of LTA, a marker of extracellular vesicles from Gram-positive bacteria, was achieved using a primary Native Lipoteichoic Acid antibody (Novus Biologicals, Cat# NBP1-60146, 1:500 dilution). Similarly, the presence of OmpA, indicative of Gram-negative bacterial extracellular vesicles, was assessed using a primary anti-Outer Membrane Protein-A antibody (Antibody Research Corporation, Cat# 111120, 1:500 dilution). EVs isolated from *Staphylococcus aureus* (Gram-positive) and *Escherichia coli* (Gram-negative) cell-culture supernatants were used as positive controls for bacterial markers. For eukaryotic-derived particles evaluation, EVs isolated from the MCF7 human cell line (12 µg), as well as EVs (40 µL) and cell lysate (obtained from 200,000 cells; 1:20 dilution) from the DI-TNC1 rat brain astrocytes cell line, were used as positive controls. Primary antibodies were used to target specific eukaryotic markers: Alix (endosomal origin marker; Cell Signalling, Cat# 2171, 1:1000 dilution), Syntenin-1 (endosomal origin marker; Abcam, Cat #ab19903, 1:1000 dilution), Flotillin-1 (membrane marker; Cell Signalling, Cat# 18634, 1:1000 dilution), TOMM20 (mitochondrial marker; Novus Biologicals, Cat# NBP2-67501, 1:1000 dilution) and Calnexin (endoplasmic reticulum marker; Abcam, Cat# ab22595, 1:1000 dilution). Secondary antibodies used included IRDye 800CW Donkey anti-Rabbit (LI-COR, Cat# 926–32213, 1:10,000 dilution), Goat anti-Rabbit Alexa Fluor Plus 800 (Invitrogen, Cat# A32735, 1:12,500 dilution), Goat anti-Rabbit Alexa Fluor 680 (Invitrogen, Cat# A21076, 1:12,500 dilution), IRDye 680RD Goat anti-Mouse (LI-COR, Cat# 926–68070, 1:10,000 dilution) and Goat anti-Mouse Alexa Fluor Plus 680 (Invitrogen, Cat# A32729, 1:12,500 dilution). Digital images of the blots were acquired using an Odyssey CLx Imaging System (LI-COR Biosciences).

To re-probe the membranes for additional proteins, a standardised stripping protocol was implemented. Briefly, membranes were incubated in 15 mL of stripping solution containing 2% (w/v) sodium dodecyl sulfate (Winkler, Cat# BM-1650), 62.5 mM Tris-HCl (pH 6.8; Winkler, Cat# BM-2000; Merck, Cat #101834) and 114.4 mM β-mercaptoethanol (Sigma-Aldrich, Cat #M3148) at 55°C for 2 h with intermittent shaking. Following this, membranes were rinsed in tap water for 2 min, washed three times for 5 min each in TBS-T (0.1%), and blocked for 1 h at room temperature using Intercept Protein-Free Blocking Buffer (LI-COR, Cat# 927–80001). Re-probing was performed with the respective primary antibodies.

2.3.4 | DNA and RNA Determination

To identify the nucleic acids contained within the bEVs, 50 µL of each sample was treated with 1 U of DNase I (Ambion, Cat# AM2222) and other 50 µL with RNase A (20 mg/mL; PureLink, Cat# 12091-021) for 30 min at 37°C to degrade all DNA and RNA present outside the vesicles. Enzymatic activity was subsequently

inactivated by adding 50 μg of Proteinase K (Invitrogen, Cat# 4485228) for 30 min at 37°C. The bEVs were then lysed using GB lysis buffer (Presto Mini gDNA Bacteria Kit, Cat# GBB004). Nucleic acid quantification was conducted with a Qubit 4 Fluorometer, employing the dsDNA HS Assay Kit (Invitrogen, Cat# Q32851 and Q32854) and RNA HS Assay Kit (Invitrogen, Cat# Q32852 and Q32855), following the manufacturer's instructions.

2.3.5 | Transmission Electron Microscopy (TEM)

bEVs image capture was performed using a Talos F200C G2 (Scanning) TEM (Thermo Fisher Scientific) at the UMA-UC Advanced Microscopy Center (Pontificia Universidad Católica de Chile, Santiago, Chile). Images were captured at 11,000× midfield and 57,000× nearfield.

2.4 | bEV Administration and Voluntary Ethanol Intake Evaluation

Two-months-old ethanol naïve Wistar rats were randomly divided into four groups (five male and five female animals per experimental group) and intraperitoneally (i.p.) injected for 3 consecutive days with: (i) 200 μL of 3% rat plasma containing 7.9×10^8 bEVs derived from the gut microbiota of UChB rats voluntarily consuming ethanol (11.4 ± 1.2 g ethanol/kg/day, mean ± SEM) for 120 days (bEVs UChB-Alcohol group); (ii) 200 μL of 3% rat plasma containing 7.9×10^8 bEVs derived from gut microbiota of ethanol-naïve UChB rats exposed to water only for 120 days (bEVs UChB-Water group); (iii) 200 μL of 3% rat plasma containing 7.9×10^8 bEVs derived from gut microbiota of Wistar rats exposed to water only for 120 days (bEVs Wistar group) and (iv) 200 μL of 3% rat plasma (vehicle group). Three percent plasma, obtained after centrifugation of blood collected via cardiac puncture in heparin-EDTA tubes from a male Wistar rat, was used to increase the protein content in the sample and prevent bEVs aggregation. One day after the last bEV administration, rats were allowed free choice access between 10% (v/v) and 20% (v/v) ethanol solutions prepared from absolute ethanol (Merck, Cat# 64-17-5) and tap water for 4 consecutive days as we previously described (three-bottle-choice test) (Ezquer et al. 2021). Ethanol and water intakes were recorded daily, and the bottle positions were alternated every day to avoid the development of side preferences. Ethanol intake was expressed as grams of ethanol consumed/kg body weight/day.

2.5 | Sample Collection for Biochemical and Immunological Analysis

Immediately after the last alcohol intake determination, animals were anesthetised with a cocktail consisting of 60 mg/kg ketamine, 10 mg/kg xylazine and 4 mg/kg acepromazine administered intramuscularly in a volume of 1.9 mL/kg. Blood samples were obtained by cardiac puncture. Then, animals were perfused intracardially with 100 mL of 0.1 M PBS (pH 7.4), as previously reported (Ezquer et al. 2021). Plasma was obtained by centrifuging 2 mL of blood at 4000 g for 10 min at 4°C. The brain was dissected as previously described (Ezquer et al. 2021) and one hemisphere was fixed in 4% paraformaldehyde (Merck, Cat# P6148) for immunofluorescence determinations, while PFC and

NAc for the other hemisphere as well as a liver sample were snap-frozen for RNA determinations.

2.6 | Quantification of Systemic Inflammation

Cytokines (IL-4, IL-1β, IL-6, IL-10, MCP-1, TNF-α, GRO and RANTES) were measured in 25 μL of plasma, using the Milliplex MAP Rat Cytokine/Chemokine Magnetic Bead Panel (Merck, Cat# RECYTMAG-65K), following the manufacturer's instructions. Data were expressed as picograms (pg) of the specific molecule/mL plasma.

2.7 | Quantification of Hepatic Inflammation

Total RNA was purified from liver samples using TRIzol (Invitrogen Cat# 15596026). One microgram of total RNA was used to perform reverse transcription with Moloney murine leukemia virus (MMLV) reverse transcriptase (Invitrogen, Cat# 28025013) and oligo-dT primers. Real-time polymerase chain reactions were made using QuantStudio 12K Flex Real-Time PCR System (Thermo Fisher Scientific) to amplify the mRNA of TNF-α, IL-6, IL-1β and LBP using the following primers: TNF-α sense: 5′-AAATGGGCTCCCTCTCATCA-3′; TNF-α antisense: 5′-TCTGCTTGGTGGTTTGCTACGAC-3′; IL-6 sense: 5′-TCCTACCCCAACTTCCAATGCTC-3′; IL-6 antisense: 5′-TTGGATGGTCTTGGTCCTTAGCC-3′; IL-1β sense: 5′-CACCTCTCAAGCAGAGCACAG-3′; IL-1β antisense: 5′-GGGTTCCATGGTGAAGTCAAC-3′; LBP sense: 5′-TGCTTCCTACATTGCTGGGG-3′; LBP antisense: 5′-TTGAAGTCCCCGCTGAAGTC-3′. Controls without reverse transcriptase during the reverse transcription reactions were included to ensure that amplicons were generated from mRNA and not from genomic DNA. Relative quantifications were performed using the ΔΔCT method. The mRNA level of each target gene was normalised against the mRNA level of the housekeeping gene β-actin in the same sample.

2.8 | Evaluation of Neuroinflammation

2.8.1 | Quantification of Proinflammatory Activated Microglia by Immunofluorescence

Microglia activation was evaluated in the PFC and the NAc by double-labelling immunofluorescence against the microglial marker ionised-calcium-binding adaptor molecule 1 (Iba-1) and the proinflammatory marker NF-κB-p65 in 30 μm thick coronal cryo-sections. Briefly, sections were washed with 0.1 M PBS (pH 7.4) and blocked for 1 h with blocking solution (0.3% Triton X-100, 0.1% BSA and 10% normal goat serum in 0.1 M PBS). Then, sections were incubated overnight at 4°C with a primary rabbit monoclonal anti-Iba-1 antibody (Cat# 019–19741, Wako, 1:500 dilution) and with a primary mouse monoclonal anti-NFκB-p65 antibody (Cat# sc-136548, Santa Cruz Biotechnology, 1:200 dilution) in Signal Stain diluent (Cat# 8112L, Cell Signalling). After that, tissue sections were rinsed with washing solution (0.1% Triton X-100 in 0.1 M PBS) and incubated for two hours at room temperature with a goat anti-rabbit Alexa Fluor 594 secondary antibody (Thermo Fisher Scientific, 1:500 dilution)

and with a goat anti-mouse Alexa Fluor 488 secondary antibody (Thermo Fisher Scientific, 1:500 dilution) in blocking solution and counterstained with DAPI (Sigma–Aldrich, 0.02 M) for nuclear labelling. Microphotographs were taken using a confocal microscope (Olympus FV10i). The area analysed for each stack was 0.04 mm^2, and each case's thickness (Z axis) was measured. Images were analysed by the FIJI image analysis software counting Iba1$^+$ cells showing nuclear staining for NF-κB-p65 as previously reported (Frakes et al. 2014).

2.8.2 | Quantification of mRNA Levels of Pro-Inflammatory Cytokines

Total RNA was purified from the PFC and NAc samples using TRIzol. One microgram of total RNA was used to perform reverse transcription with MMLV reverse transcriptase and oligo-dT primers. Real-time polymerase chain reactions were made using QuantStudio 12K Flex Real-Time PCR System (Thermo Fisher Scientific) to amplify the mRNA of IL-1β, IL-6 and TNF-α. Relative quantifications were performed using the $\Delta\Delta$CT method. The mRNA level of each target gene was normalised against the mRNA level of the housekeeping gene β-actin in the same sample.

2.8.3 | Quantification of Proinflammatory Activated Microglia by Flow Cytometry

After cardiac perfusion, the brain tissue was collected and dissociated to obtain viable single-cell suspensions. The cortical tissue was placed in cTubes (Miltenyi) containing a papain-based solution (3 U/mL papain (Sigma–Aldrich), 10 mM HEPES (Gibco), 5% FBS (Gibco) in HBSS with Ca^{+2} and Mg^{+2} (Gibco)) and processed with the *m_brain_01* program on the gentleMACS Dissociator (Miltenyi). After 15 min of incubation at 37°C with rotation, the tissue was further dissociated using the *m_brain_02* program. DNAse I (ThermoFisher Scientific Cat# EN0521, 20,000 U/mL, 30 µL) was then added to digest released DNA, followed by a 10-min incubation at 37°C with rotation. The suspension was processed again with the *m_brain_03* program and incubated for 10 min at 37°C. The dissociated tissue was filtered through a 70 µm cell strainer (Falcon), washed with HBSS (300 × g, 10 min, 4°C), and resuspended in 3.1 mL cold PBS. Myelin was removed by layering 4 mL cold PBS over 900 µL Debris Removal Solution (Miltenyi) to form a gradient, which was centrifuged (3000 × g, 10 min, 4°C, swing-out rotor). After discarding the supernatant containing the myelin band, the cell pellet was washed with PBS (1000 × g, 10 min, 4°C) and resuspended in FACS buffer (PBS, 2% FBS, 0.5 mM EDTA). Cells were stored on ice until staining.

Microglial activation was assessed by evaluating phenotypic and activation markers using flow cytometry. Viability was determined with the LIVE/DEAD Fixable Near IR (1:2,000). Surface marker CD11b/c (PerCP-Cy5.5, Biolegend, Cat# 201820, 1:400) and intracellular marker CD68 (FITC, Invitrogen, Cat# MA528262, 1:100) were employed, with intracellular staining performed using the eBiosciences Fixation/Permeabilisation Kit (eBiosciences). For staining, 1×10^6 cells were incubated with the viability dye for 15 min at room temperature in the dark,

washed twice with FACS buffer (600 × g, 5 min) and labelled with anti-CD11b/c for 30 min at 4°C. After washing, cells were fixed, permeabilised and stained with anti-CD68 for 90 min at 4°C. Following two washes, cells were resuspended in 150 µL FACS buffer and analysed on a Cytek Aurora cytometer. Data were analysed using FlowJo software (Ashland, Oregon, USA). Live cells were gated based on FSC versus SSC and viability staining (see Figure S6 for gating strategy). As a positive control for neuroinflammation animals were i.p. injected with 5 mg/kg LPS (Sigma-Aldrich Cat# L3755) or the vehicle, and 16 h later the brain cortices were processed as previously indicated.

2.9 | Subdiaphragmatic Vagotomy and Evaluation of Ethanol Intake

To evaluate the role of the vagus nerve in bEV-induced ethanol intake, 2-month-old male Wistar rats were subjected to subdiaphragmatic vagotomy as previously described (Ezquer et al. 2021). Briefly, animals were anesthetised with a cocktail consisting of 60 mg/kg ketamine, 10 mg/kg xylazine and 4 mg/kg acepromazine administered intramuscularly in a volume of 1.9 mL/kg. A midline laparotomy was performed to expose the stomach and lower esophagus. The left lateral lobe of the liver was retracted to visualise the distal end of the esophagus. A ligature was placed around the esophagus at its entry into the stomach to allow gentle retraction to expose both vagal branches. Using jeweler's forceps, both branches of the vagus nerve were isolated from the esophagus, and a 2-mm section of each nerve branch was resected. In the case of the sham animals, vagal branches were similarly exposed but left intact. Following nerve manipulation, the incisions were closed. All animals were kept under special postsurgical care for 3 days, and an 11-day recovery period was allowed before bEVs administration. Vagotomised Wistar animals were administered bEVs from UChB-Alcohol rats either by i.p. injection or by oral gavage (Vagotomy bEVs UChB-Alcohol). Sham operated animals received either bEVs from UChB-Alcohol rats (Sham bEVs UChB-Alcohol) or vehicle (Sham Vehicle) via i.p. injection or by oral gavage. bEV doses were 7.9×10^8 particles in total suspended in 3% rat plasma, regardless of the delivery route tested. Final delivery volumes were 200 µL for i.p. injection and 1 mL for oral gavage. The animals received a daily bEV administration for 3 consecutive days. One day after the last bEV administration (i.p. or oral gavage), rats were allowed free choice access between 10% (v/v) and 20% (v/v) ethanol solutions prepared from absolute ethanol (Merck) and tap water for 4 consecutive days as previously described (three-bottle-choice test) (Ezquer et al. 2021).

2.10 | Statistical Analysis

Statistical analyses were performed using GraphPad Prism software (V.10.2.0 San Diego, CA, USA). Data are expressed as mean ± SEM. The normal distribution of data was first tested using Shapiro-Wilk test. For normal distributed data, one-way or two-way analysis of variance (ANOVA) was used followed by Tukey or Dunnett post hoc tests. Conversely Kruskal–Wallis analysis was performed for nonparametric data. A level of $p < 0.05$ was used for statistical significance.

3 | Results

3.1 | Characterisation of Gut Microbiota Composition

The gut microbiota composition across the three different donor animal groups was analysed at the outset. For this, 16S rRNA sequencing was applied to detect the microbiota profile in faeces collected from: (i) UChB rats voluntarily consuming a 10% ethanol solution for 120 days (UChB-Alcohol group), (ii) UChB rats consuming only water (UChB-Water group) and (iii) Wistar rats consuming only water (Wistar group). Richness within samples (α-diversity) showed no statistical differences between groups when analysed using the Chao 1 and Shannon indices (Figure 1A). However, β-diversity analysis revealed significant differences between the three experimental groups, as shown by Principal Coordinate Analysis (PCoA) (PERMANOVA analysis, $p = 0.002$; Figure 1B). Relative abundance between experimental groups was analysed at the phylum (Figure 1C), class (Figure 1D), family (Figure 1E) and genus (Figure 1F) levels. Several phyla, classes and families showed statistical abundance differences between groups, including Verrucomicrobiota, Bacteroidia and Clostridiaceae, respectively (Kruskal–Wallis, Table S1). However, we focused the analysis on abundances that were similar between the UChB-Alcohol and UChB-Water groups while being distinct from those of the Wistar group, as these two microbiota compositions are known to promote drinking behaviour in UChB animals (Ezquer et al. 2021, 2022). At the family level, Acidaminococcaceae showed a higher relative abundance in both UChB groups compared to Wistar animals ($p = 0.021$), while Anaerovoracaceae ($p = 0.002$), Turicibacteraceae ($p = 0.025$) and Coriobacteriaceae ($p = 0.002$) showed lower relative abundance in both UChB groups compared to Wistar group (Figure 1E). At the genus level, *Limosilactobacillus* ($p = 0.004$), *Phascolarctobacterium* A ($p = 0.02$), *Prevotella* ($p = 0.02$) and *Butyricicoccus A* ($p = 0.004$) had lower relative abundances in the Wistar group compared to the UChB-Water and UChB-Alcohol groups. In contrast, *Romboutsia E* ($p = 0.0015$) and *F23-B02* ($p = 0.003$) showed higher relative abundance in the Wistar group compared to the UChB-Water and UChB-Alcohol groups (Figure 1F). A full comparison of the more abundant taxa across the three experimental groups is presented in Figure S1.

3.2 | Characterisation of Gut Microbiota-Derived bEVs

Gut microbiota-derived particles were obtained from freshly collected stool samples sourced from the three different origins. Figure 2A illustrates a schematic representation of the methodology employed for isolating EVs. Following isolation, the particles were characterised following the guidelines described in the MISEV2023 recommendations (Welsh et al. 2024).

Nanoparticle tracking analysis confirmed the successful isolation of particles, showing a consistently high particle concentration across all groups, with peaks in the size range of 150–400 nm (Figure 2B). The particle size distributions exhibited non-symmetric unimodal profiles with positively skewed curves, consistent with the expected size range for bacterial vesicles (20–400 nm) (Haas-Neill and Forsythe 2020). The average particle

concentration derived from five independent isolations for the Wistar group was $2.7 \times 10^{11} \pm 8.42 \times 10^{10}$ particles/mL, while the UChB-Water and UChB-Alcohol groups yielded $1.99 \times 10^{11} \pm 7.28 \times 10^{10}$ particles/mL (six independent isolations) and $4.22 \times 10^{11} \pm 8.42 \times 10^{10}$ particles/mL (nine independent isolations), respectively. The mode particle sizes were 214.7 ± 8.5 nm for Wistar, 240.8 ± 12.9 nm for UChB-Water and 225.9 ± 9.1 nm for UChB-Alcohol. No statistically significant differences were observed in particle concentration or size among the experimental groups (Figure 2C). However, the UChB-Alcohol group showed a trend toward higher particle concentration compared to the other groups, potentially reflecting the impact of alcohol consumption on vesicle production.

As shown in Figure 2D,E, a deeper characterisation of bEVs confirmed their bacterial origin through the detection of specific protein markers and LPS content. Quantification of LPS, a hallmark component of the outer membrane of Gram-negative bacteria, revealed a trend toward reduced levels in the UChB-Alcohol group ($4.97 \times 10^{-8} \pm 2.36 \times 10^{-8}$ EU/particle) compared to the UChB-Water ($1.11 \times 10^{-7} \pm 3.93 \times 10^{-8}$ EU/particle) and Wistar groups ($1.07 \times 10^{-7} \pm 4.08 \times 10^{-8}$ EU/particle). Western blot analysis further confirmed the bacterial origin of the vesicles by detecting LTA, a major cell wall polymer found in Gram-positive bacteria, in all samples. Additionally, OmpA, a well-established marker of Gram-negative bEVs, was consistently present in all groups. The combined analysis of LPS quantification and protein markers indicates that the isolated bEVs include vesicles originating from both Gram-positive and Gram-negative bacteria.

Given that the term 'microbiota' specifically refers to microorganisms and excludes host or environmental components, we conducted an additional analysis to evaluate the potential presence of eukaryotic EVs derived from donor rats. This analysis was critical to ensure that the observed behavioural results were primarily attributable to bEVs. Western blot analysis was performed to detect eukaryotic EV markers, including Alix, Flotillin-1 and Syntenin-1, as well as non-EV eukaryotic cell markers such as Calnexin (endoplasmic reticulum marker) and TOMM20 (mitochondrial marker). As shown in Figures 2E and S2, no signal was observed for any of the eukaryotic markers tested, indicating an undetectable presence of donor-derived EVs in the bEV samples.

The nucleic acid composition of the isolated bacterial bEVs was also quantified, confirming the presence of both DNA and RNA, with levels potentially influenced by sample source and alcohol consumption (Figure 2F). Specifically, bEVs derived from the gut microbiota of Wistar rats contained 8.6 ng of DNA and 214 ng of RNA, corresponding to 1.39 ng of DNA and 34.79 ng of RNA per 1×10^9 particles. In comparison, bEVs from UChB rats consuming water showed 7.6 ng of DNA and 123 ng of RNA, resulting in 1.37 ng of DNA and 22.16 ng of RNA per 1×10^9 particles. bEVs from UChB rats consuming alcohol exhibited the highest nucleic acid content, with 12.3 ng of DNA and 225 ng of RNA, equating to 1.67 ng of DNA and 30.61 ng of RNA per 1×10^9 particles.

To confirm the presence, morphology and structural integrity of the vesicles, samples were analysed by TEM. The vesicles isolated from the three experimental rat groups exhibited high
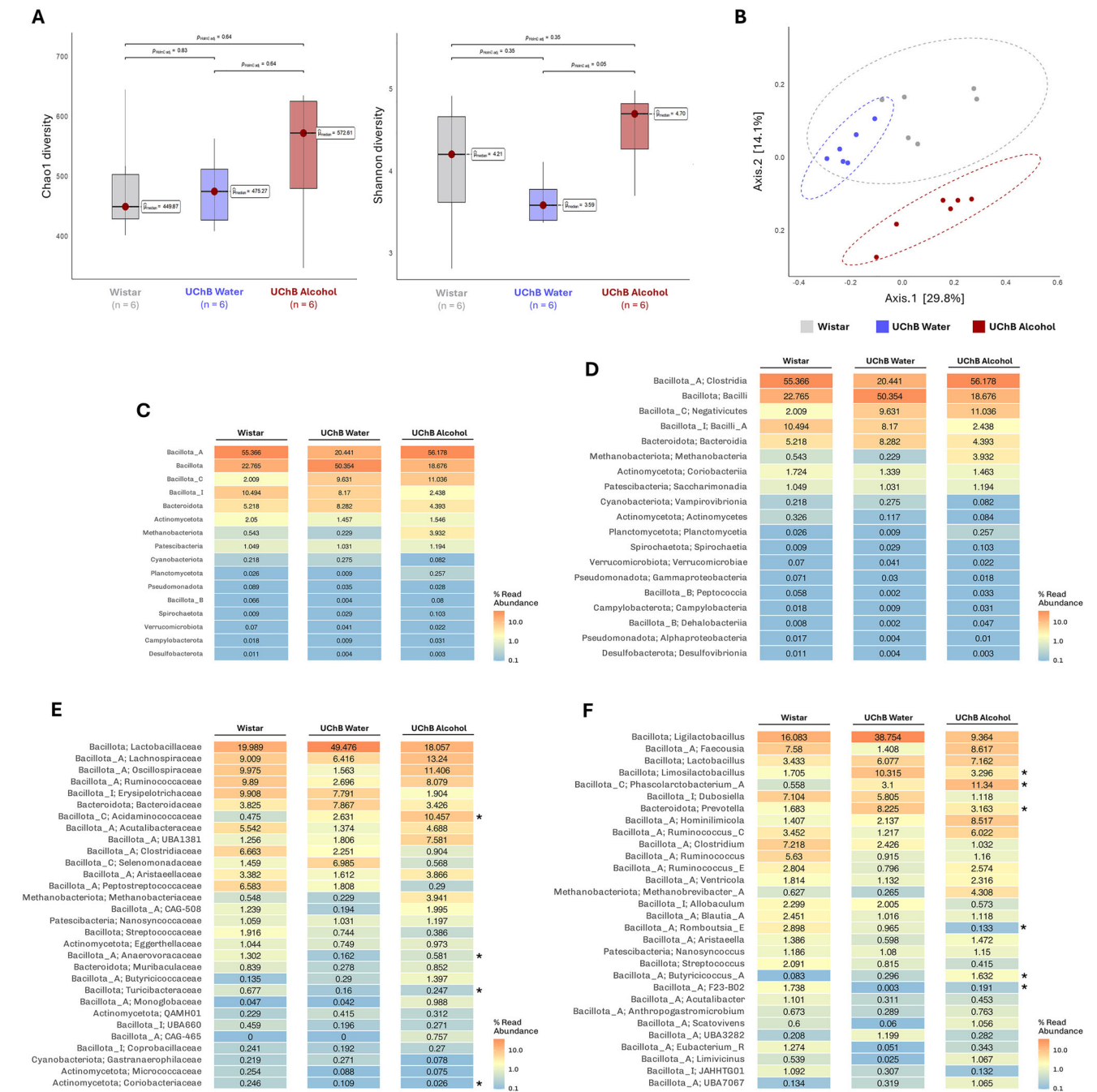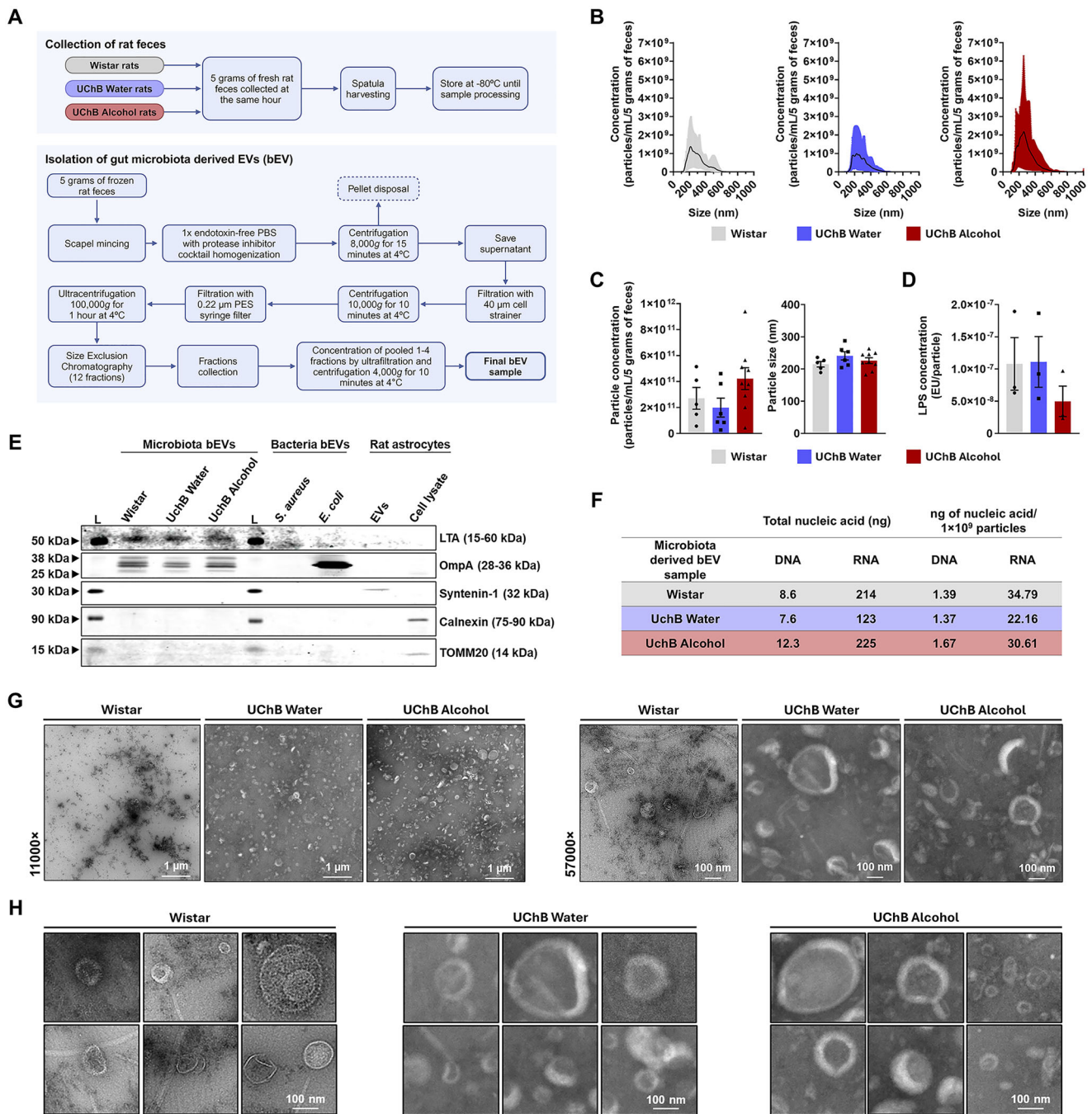
FIGURE 1 | Gut microbiota characterisation of bEV donor animal groups. (A) Chao-1 and Shannon diversity indices of faeces collected from Wistar, UChB-Water and UChB-Alcohol animals. No statistical differences were detected between groups in α-diversity indices, as determined by nonparametric pairwise multiple comparisons (Kruskal–Wallis and Dunn's test). $n = 6$ per experimental group. (B) Principal Coordinates Analysis (PCoA) plot of β-diversity based on Bray-Curtis dissimilarities. Each dot represents a unique faecal sample from a single animal. Wistar, UChB-Water and UChB-Alcohol animals clustered significantly different (PERMANOVA analysis, $p = 0.002$). $n = 6$ per experimental group. (C) Relative abundance at the phylum level. (D) Relative abundance at the class level. (E) Relative abundance at the family level. (F) Relative abundance at the genus level. Kruskal–Wallis analysis, * shows $p < 0.05$ only when UChB-Water and UChB-Alcohol abundances are similar and at the same time different from Wistar abundance. $n = 6$ per experimental group.

structural integrity, displaying a wide range of sizes and electron density profiles (Figure 2G). TEM images revealed vesicles with characteristic spherical and cup-shaped morphologies, consistent with bEVs. Interestingly, a variety of vesicle morphologies were observed (Figure 2H), reflecting the microbial diversity within the intestinal microbiota of the experimental groups. Notably, vesicles from the UChB-Alcohol group appeared to differ structurally from those in the Wistar and UChB-Water groups, showing an increased electron density and a greater number of vesicles per field.

FIGURE 2 | Characterisation of gut microbiota-derived bEVs. (A) Schematic representation of the procedure used for collecting animal faeces and the protocol for isolating EVs. The enrichment of microbiota-derived bEVs was conducted using a protocol combining multiple filtration steps, centrifugations and size exclusion chromatography (SEC). (B) Size distribution and (C) total particle concentration and mode of particle size were evaluated by Nanoparticle Tracking Analysis (NTA). (D) Quantification of lipopolysaccharide (LPS) by spectrophotometry of isolated particles (EU = endotoxin units). (E) Western blot analysis of isolated EVs revealed the presence of lipoteichoic acid (LTA, Gram-positive bacteria marker) and outer membrane protein-A (OmpA, Gram-negative bacteria marker). Note that there is no detectable presence of eukaryotic proteins Syntenin-1 (endosomal EV-origin marker), Calnexin (endoplasmic reticulum marker) and TOMM20 (mitochondria marker) (L = molecular weight ladder). (F) Determination of DNA and RNA presence in bEVs showing measured nucleic acid content and normalised nucleic acid content per 1×10^9 particles. (G) Representative Transmission Electron Microscopy (TEM) micrographs of bEVs samples. (H) Micrograph panels depicting a plethora of EVs morphologies derived from the gut microbiota. Data are presented as mean ± SEM.

Altogether, these results confirm that bEVs with high integrity were successfully isolated from the three experimental rat groups, exhibiting sizes and markers indicative of bacterial vesicles.

3.3 | Gut Microbiota-Derived bEVs of Both UChB-Alcohol and UChB-Water Animals Trigger High Voluntary Alcohol Consumption in Alcohol-Rejecting Wistar Rats

To study the impact of bEVs derived from UChB gut microbiota on alcohol consumption in alcohol-rejecting Wistar rats, four groups of adult ethanol-naïve male Wistar rats were i.p. injected with 7.9×10^8 bEVs isolated from the three different origins or with the vehicle for 3 consecutive days, and a 4-day assessment of alcohol intake using a three-bottle-choice test was performed 1 day after the last bEVs administration (Figure 3A). Both Wistar rat groups that received UChB-derived vesicles exhibited a continuous increase in alcohol consumption over the 4 days of free ethanol access, starting from the first day of assessment (Figure 3B). Wistar rats i.p. injected with UChB-Alcohol bEVs significantly increased their voluntary alcohol consumption compared to the vehicle-injected group, reaching a maximum alcohol intake of 4.95 ± 0.36 g ethanol/kg/day 4 days after the last bEV administration, representing ~10-fold increase in ethanol intake compared to vehicle-injected rats ($p < 0.001$) (Figure 3B). Similarly, Wistar rats receiving UChB-Water bEVs also showed a significant increase in alcohol consumption compared to the vehicle-injected animals, reaching an alcohol intake of 4.71 ± 0.36 g ethanol/kg/day 4 days after the last bEV administration ($p < 0.001$) (Figure 3B). On the first day of ethanol intake, the increase in ethanol consumption of animals that received bEVs from UChB-Water animals showed an apparent delay compared to animals that received bEVs from UChB-Alcohol animals. Notably, there was no statistical difference in the maximum amount of alcohol consumed by the Wistar rats injected with UChB-Alcohol bEVs or UChB-Water bEVs, thus highlighting the potency of innate microbiota of the UChB strain in promoting voluntary alcohol intake. Conversely, Wistar rats injected with Wistar-derived bEVs reached a maximum alcohol consumption of 0.44 ± 0.43 g ethanol/kg/day, showing no increase in alcohol intake compared to the vehicle-injected group (maximum alcohol intake of 0.65 ± 0.36 g ethanol/kg/day) (Figure 3B).

Previous reports indicate that susceptibility to high alcohol intake differs between males and females in both human and animal models, with females being more prone to high alcohol consumption (Dhaher et al. 2012; Loi et al. 2014). To evaluate whether the sex of the recipient animals could influence the behavioural effects related to alcohol intake, four groups of adult ethanol-naïve female Wistar rats were i.p. injected with the different bEVs, following the same experimental design shown in Figure 3A. As previously observed in male Wistar rats, female Wistar rats that received UChB-Water and UChB-Alcohol bEVs significantly increased their alcohol consumption over the 4 days of free ethanol access, starting from the first day of assessment, compared to female rats receiving Wistar-derived bEVs (Figure 3C). Once again, no significant differences were

observed in the maximum amount of alcohol consumed by female Wistar rats injected with UChB-Alcohol bEVs (10.38 ± 2.02 g ethanol/kg/day 4 days after the last bEV administration) or UChB-Water bEVs (11.77 ± 2.62 g ethanol/kg/day 4 days after the last bEV administration). However, female Wistar rats voluntarily consumed more than double the amount of alcohol compared to male rats after receiving the i.p. administration of UChB-derived bEVs, representing an almost 50-fold increase compared to vehicle-injected female animals (Figure 3C). Neither animal weight nor total fluid intake was altered by bEV administration in male or female Wistar rats (Figure S3A-D), suggesting that the observed behavioural effect is attributable to the bEV injection.

These results suggest that: (i) gut microbiota-derived bEVs are enough to transmit alcohol preference between different rat strains without bacteria needing to colonize the gut; (ii) not all bEVs can promote drinking behaviour; therefore, a specific combination of bacterial source and bEVs cargo composition is required to induce alcohol intake in injected animals and (iii) female rats voluntarily consumed more alcohol than male rats following the i.p. administration of UChB-derived bEVs.

3.4 | Systemic and Liver Inflammation Were Not Detected in bEV-Injected Wistar Rats That Acquire a High Alcohol Intake

Inflammation has been strongly linked to high drinking behaviour (Blednov et al. 2011; Koob and Volkow 2016). To investigate whether the elevated alcohol consumption in animals injected with UChB-bEVs was triggered by a systemic inflammatory process induced by bEV administration, immediately after the 4th day of voluntary alcohol intake evaluation the plasma levels of eight cytokines (IL-4, IL-1β, IL-6, TNF-α, MCP-1, RANTES, GRO and IL-10) associated with systemic inflammation was evaluated using the MILLIPLEX multiplex immunoassay. As shown in Figure 4A, animals injected with the different types of bEVs showed no significant differences in any of the evaluated cytokines compared to the vehicle-injected group ($p > 0.05$). This suggests that, even though all isolated bEV types contain LPS (Figure 2D), the delivered amount of LPS was insufficient to trigger a detectable systemic inflammation. Consequently, the increase in voluntary alcohol consumption observed in Wistar rats injected with bEVs isolated from the microbiota of both UChB-Alcohol and UChB-Water rats appears triggered independently of a systemic inflammatory process.

As gut microbiota metabolites can also induce liver inflammation (Mayfield et al. 2013), we analysed pro-inflammatory markers in the liver tissue collected immediately after the 4th day of voluntary alcohol intake evaluation. RNA levels of TNF-α, IL-6, IL-1β and lipopolysaccharide binding protein (LBP) were measured by RT-qPCR. However, no differences between the experimental groups in the expression levels of these proinflammatory markers were detected ($p > 0.05$), suggesting that liver inflammation is not necessary to increase voluntary alcohol intake (Figure 4B).
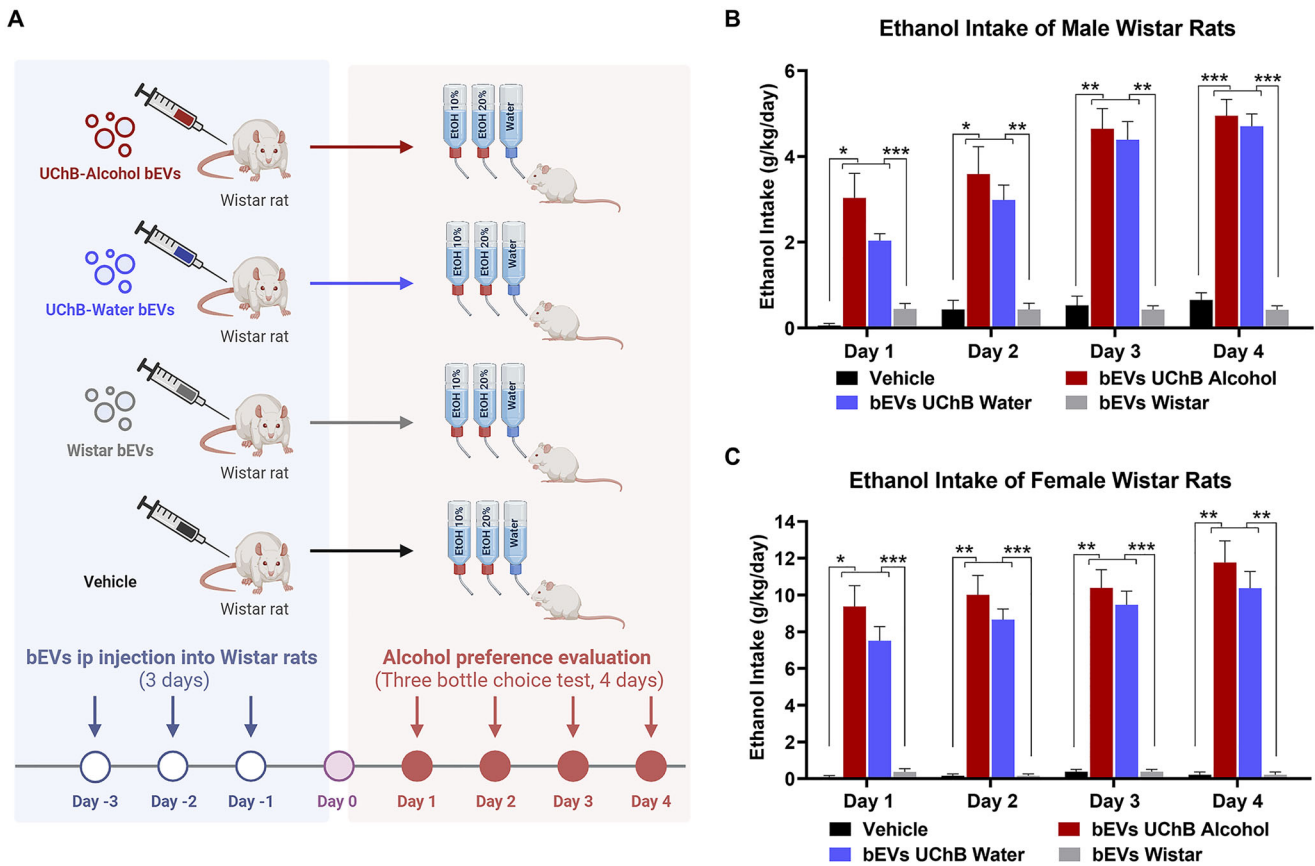
FIGURE 3 | Innate gut microbiota-derived bEVs from UChB rats induce high voluntary alcohol consumption in male and female alcohol-rejecting Wistar rats. (A) Schematic representation of methodology for animal groups and interventions. Male and female ethanol-naïve Wistar rats received either a dose of bEVs (containing 7.9×10^8 bEVs resuspended in 3% of rat plasma) or a vehicle via i.p. injection during 3 consecutive days. The following day, each animal was given concurrently free choice between ethanol 10% (v/v), ethanol 20% (v/v) or tap water. This three-bottle-choice consumption test was performed for 4 consecutive days and then animals were euthanised. (B) Daily voluntary ethanol intake of male Wistar rats i.p. injected with bEVs or vehicle. Ethanol consumption was calculated as grams of ethanol per kilogram of rat per day. Two-way analysis of variance (ANOVA) (treatment × day) of all data shown in Figure 2B revealed a significant effect of treatment [$F_{treatment}$ (3,16) = 45.58, $p < 0.0001$], days [F_{day} (2.412, 38.59) = 49.72, $p < 0.0001$], and significant treatment × day interaction [$F_{interaction}$(9, 48) = 11.89, $p < 0.0001$] versus the control group injected with vehicle. Tukey post hoc analysis indicated that bEVs derived from gut microbiota of UChB rats that had ingested alcohol for 120 days induced a significant increases of ethanol intake of Wistar rats on Days 1, 2 ($p < 0.05$), 3 ($p < 0.01$) and 4 ($p < 0.001$) versus that of the control group injected with vehicle. Further, post hoc analysis indicated that bEVs derived from the gut microbiota of UChB-Water rats also induced a significant increases ethanol intake of Wistar rats on Days 1 ($p < 0.001$), 2 ($p < 0.05$), 3 and 4 ($p < 0.0001$) versus that of the control group injected with vehicle and versus that of the group bEVs isolated from Wistar strain ($p < 0.05$ on Days 1 and 2, $p < 0.01$ on Day 3 and $p < 0.001$ on Day 4). (C) Daily voluntary ethanol intake of female Wistar rats i.p. injected with bEVs or vehicle. A two-way analysis of variance (ANOVA) (treatment × day) of all data shown in Figure 2C revealed a significant effect of treatment [$F_{treatment(3,16)}$ = 87.32, $p < 0.0001$], day [$F_{day(1737,27.80)}$ = 8.476, $p < 0.002$] and a significant treatment day interaction [$F_{interaction(9,48)}$ = 3.377, $p < 0.0028$] compared to the vehicle group. Tukey post hoc test indicated that the i.p. administration of bEVs derived from the gut microbiota of either UChB water-drinking or UChB alcohol-drinking rats significantly increased voluntary ethanol intake in female Wistar rats (*$p < 0.05$; **$p < 0.01$; ***$p < 0.001$). Data are presented as mean ± SEM; $n = 5$ per experimental group.

3.5 | Neuroinflammation Was Not Detected in bEV-Injected Wistar Rats That Acquire a High Alcohol Intake

We further evaluated inflammation directly in brain tissue. Microglia are considered the primary cell type in the brain parenchyma responsible for producing proinflammatory molecules (Jurga et al. 2020). Thus, to assess pro-inflammatory microglial activation, we performed immunofluorescence analysis in the PFC and NAc, two brain areas where neuroinflammation has been previously linked to alcohol addiction (Erickson et al. 2021; Everitt and Robbins 2005).

Iba-1^{+} cells showing nuclear staining for NF-κB-p65—a classical marker of pro-inflammatory activation (Frakes et al. 2014)—were quantified. Surprisingly, we observed no changes in the frequency of Iba-1^{+}/nuclear NF-κB-p65^{+} cells or in the total number of nuclear NF-κB-p65^{+} cells in the PFC (Figures 5A, S4 and S5A) and NAc (Figures 5B, S4 and S5B) under any experimental conditions, suggesting that bEV administration does not induce pro-inflammatory microglia activation.

To further confirm these results, we measured the expression levels of the classical pro-inflammatory cytokines IL-1β, IL-6 and TNF-α by RT-qPCR in both brain regions. No significant changes
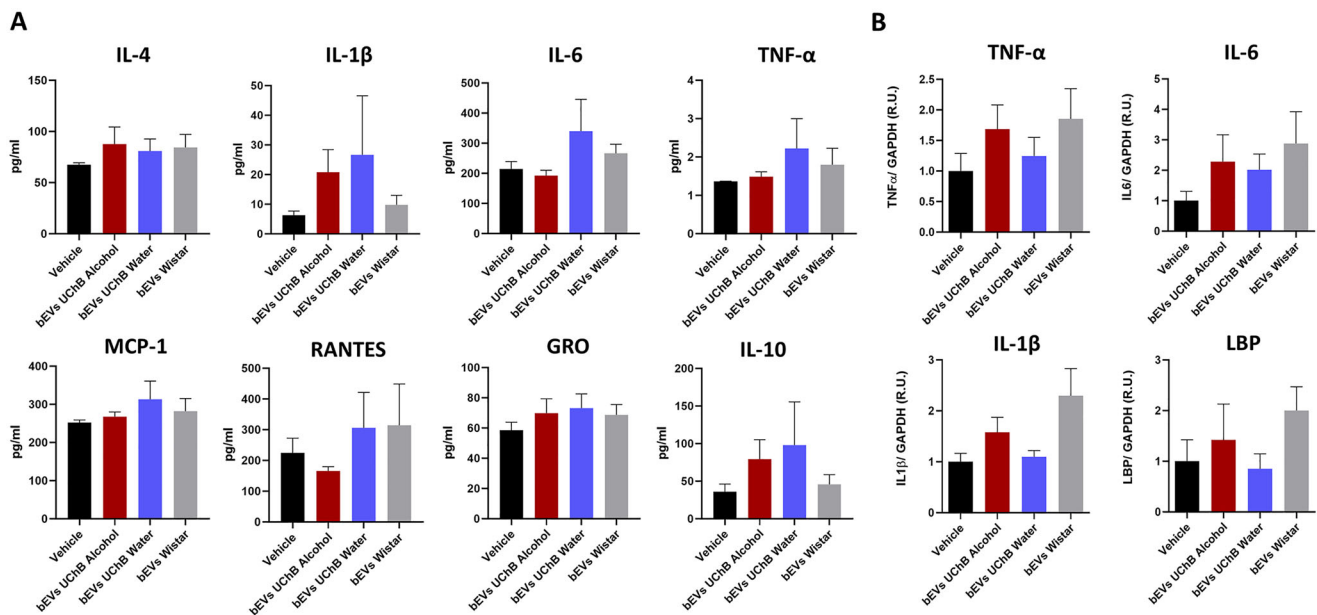
FIGURE 4 | Gut microbiota-derived bEVs do not trigger detectable systemic or liver inflammation. (A) Plasmatic levels of IL-4, IL-1β, IL-6, TNF-α, MCP-1, RANTES, GRO and IL-10 of euthanised animals measured by MILLIPLEX Panel revealed no differences between bEVs-injected groups and vehicle. One-way ANOVA and Dunnett's test, $p > 0.05$. Data are shown as mean and SEM; $n = 5$ per group. (B) RNA levels of the pro-inflammatory cytokines TNF-α, IL-6, IL-1β and LBP show that bEV treatment had no significant impact on liver inflammatory status. One-way ANOVA and Dunnett's test, $p > 0.05$. Data are shown as mean $\pm$ SEM; $n = 5$ per experimental group.

in the levels of these proinflammatory molecules were observed in bEV-treated animals compared to vehicle-treated animals in both brain regions (Figure 5C). Finally, to further assess microglial activation, the expression of an activation marker was evaluated by flow cytometry in single-cell suspensions obtained from the dissociated brain cortices of the animals. Living cells were labelled for CD11b/c as a marker of microglia and for CD68 as a marker of pro-inflammatory activation. Once again, we found no statistically significant differences in the frequency of activated microglia (CD11b/c^{+} CD68^{+} cells, gating strategy in Figure S6A) across experimental groups (Figure 5D,E), nor in the percentage of microglial cells of total living cells (Figure S6B). As a positive control for neuroinflammation, animals were intraperitoneally injected with 5 mg/kg LPS or the vehicle (Skrzypczak-Wiercioch and Salat 2022). As expected, LPS administration induced a marked increase in the frequency of CD68^{+} activated microglia compared to vehicle treated animals (Figure S6C). Taken together, these results strongly suggest that bEV administration does not induce neuroinflammation in the PFC and NAc of recipient animals.

3.6 | Vagotomy Inhibits Voluntary Ethanol Consumption Induced by the Administration of UChB-Derived bEVs

Since neuroinflammation was not detected, we evaluated the role of another key component of the gut-brain axis: the vagus nerve. The vagus nerve is the main neuronal communication route between gut bacteria and the CNS (Cryan and Dinan 2012; Leclercq et al. 2017), and due to its long extension, it is systemically exposed. Therefore, we were interested in assessing the vagus nerve's role in mediating the communication between

the administered bEVs and the brain. For this, subdiaphragmatic bilateral vagotomy was carried out in Wistar animals, while sham surgery was performed as a control. bEVs derived from the microbiota of UChB-Alcohol animals—which emulates the human fecal microbiota of AUD patients—or the vehicle were i.p. injected, and voluntary alcohol consumption of Sham-Vehicle, Sham-UChB-Alcohol bEVs or Vagotomy-UChB-Alcohol bEVs groups was evaluated by the three-bottle-choice test (Figure 6A). As expected, animals in the sham group i.p. injected with bEVs derived from the gut microbiota of UChB-Alcohol animals significantly increased their voluntary alcohol intake compared to sham animals injected with the vehicle ($p < 0.01$) (Figure 6B). Remarkably, vagotomy completely abolished the bEVs effect on ethanol intake, since vagotomised animals decreased their alcohol intake by 97.9% compared to the sham group injected with bEVs ($p < 0.01$) (Figure 6B). There was no difference in alcohol consumption between the Vagotomy-UChB-Alcohol bEVs group and the Sham-Vehicle group, demonstrating a key role of the vagus nerve in bEVs-mediated communication with the brain. Given the robustness of this result, we wondered whether vagotomy would have the same effect if bEVs were delivered via oral gavage, a delivery route that better simulates the natural location of bEV generation. To test this, we first evaluated the voluntary alcohol consumption of animals gavaged with bEVs. We delivered the same dose of bEVs (7.9×10^8) or vehicle used in the intraperitoneal design. Surprisingly, animals that received bEVs via oral gavage consumed a similar amount of ethanol compared to those injected with bEVs intraperitoneally, albeit with different kinetics (Figure 6C). Ethanol consumption was higher on Day 1 (4.90 ± 2.21 g ethanol/kg/day) compared to Day 2 (3.77 ± 1.74 g ethanol/kg/day), increasing up to Day 4, when it peaked at 6.19 ± 2.01 g ethanol/kg/day. This consumption was significantly higher than that of the vehicle group ($p < 0.05$). After
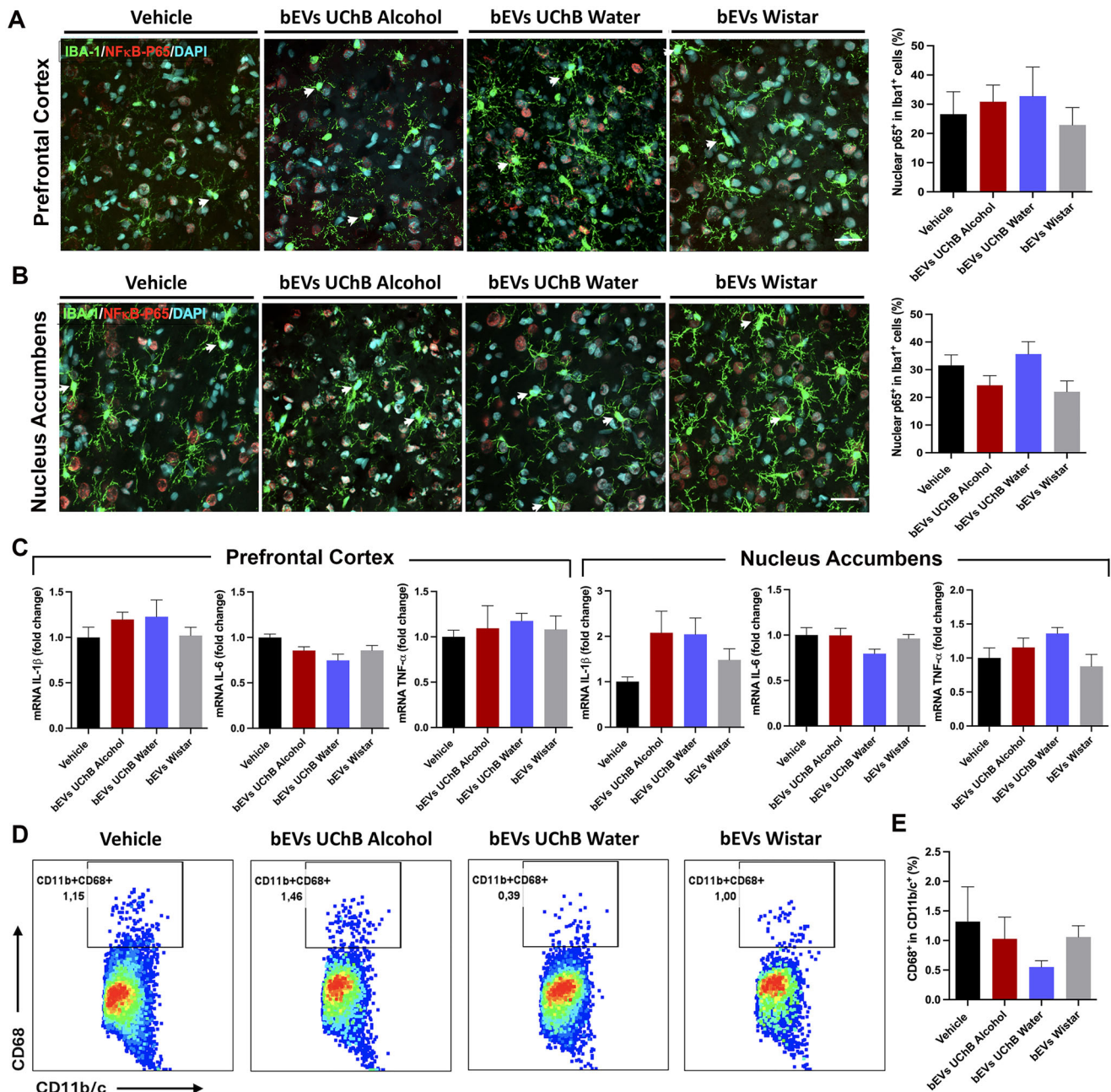
FIGURE 5 | Gut microbiota-derived bEVs do not trigger detectable neuroinflammation. (A) Representative confocal microscopy microphotographs of microglial cells labelled for the Iba-1 marker (green) and the pro-inflammatory activation marker NF-κB-p65 (red) to evaluate activated microglia (white arrows) in Prefrontal Cortex (PFC) and (B) Nucleus Accumbens (NAc). Nuclei were stained with DAPI (blue). Microglia activation was assessed as the percentage of Iba1$^+$ cells showing nuclear staining for NF-κB-p65. Data indicated no significant differences between the bEV-injected groups and the vehicle-injected group. Data are shown as mean ± SEM. One-way ANOVA and Dunnett's test, $p > 0.05$ $n = 5$ per group. Scale bar = 30 μm. (C) RNA levels of pro-inflammatory cytokines IL-1β, IL-6 and TNF-α in the PFC and NAc show that bEVs treatment had no significant impact on classical pro-inflammatory cytokine production in both brain regions. One-way ANOVA and Dunnett's test, $p > 0.05$. Data are presented as mean ± SEM; $n = 5$ per experimental group. (D) Representative dot plots of CD11b/c$^+$CD68$^+$ cells determined from brain cortices of bEV and vehicle-treated animals. (E) Comparison of the percentage of CD68$^+$ cells of total CD11b/c$^+$ cells between brain cells of different experimental groups. Data indicated no significant differences between the bEV-injected groups and the vehicle-injected group. Data are shown as mean ± SEM. One-way ANOVA and Dunnett's test, $p > 0.05$ $n = 5$ per group.

confirming that oral gavage of UChB-Alcohol bEVs increased alcohol consumption in Wistar rats, we assessed the role of the vagus nerve in this effect. We repeated the experimental design shown in Figure 6A, including Sham-Vehicle, Sham-UChB-Alcohol bEVs and Vagotomy-UChB-Alcohol bEVs groups.

Once again, vagotomy significantly reduced alcohol consumption when comparing the Sham-UChB-Alcohol bEVs group to the Vagotomy-UChB-Alcohol bEVs group ($p < 0.05$), resulting in a 92% reduction in the effect of orally gavaged bEVs in vagotomised animals (Figure 6D). Taken together, these findings
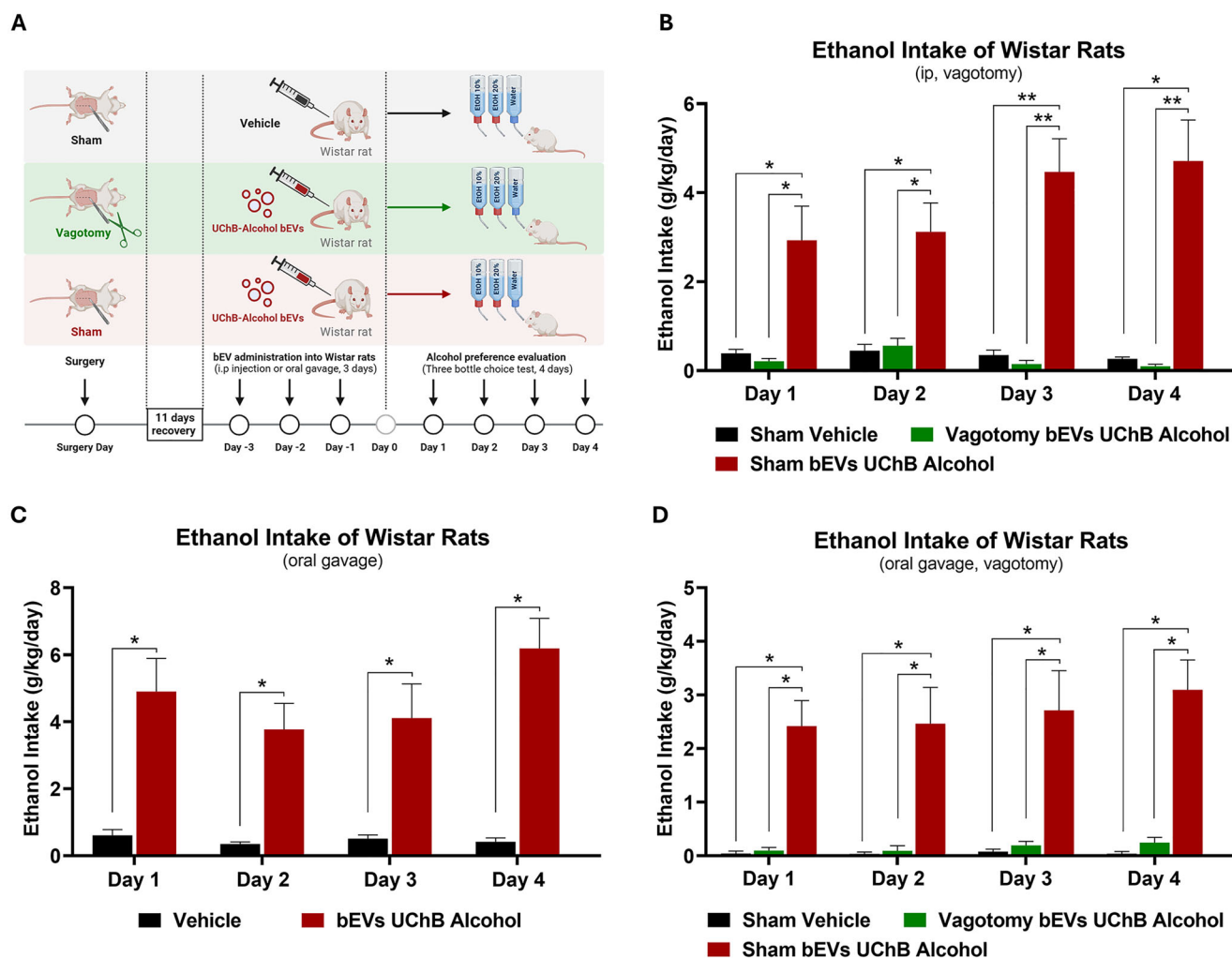
FIGURE 6 | Vagotomy inhibits voluntary ethanol consumption induced by bEVs derived from gut microbiota of UChB rats that had drunk ethanol. (A) Schematic representation of methodology for animal groups and interventions. After undergoing either subdiaphragmatic vagotomy or sham surgery, Wistar rats received bEVs isolated from UChB-Alcohol rats (7.9×10^8 bEVs) or the vehicle via i.p. injection or by oral gavage for 3 consecutive days. The following day, each animal was given concurrently free choice between ethanol 10% (v/v), ethanol 20% (v/v) or tap water. This three-bottle-choice consumption test was performed for 4 consecutive days and then animals were euthanised. (B) Daily ethanol intake of vagotomised or sham-operated animals treated by the i.p. administration of bEVs isolated from UChB-Alcohol rats. Ethanol consumption was calculated as grams of ethanol per kilogram of rat per day. Two-way analysis of variance (ANOVA) revealed a significant effect of vagotomy [$F_{treatment(2,15)} = 21.50$, $p < 0.0001$], day [$F_{day(2259,33.88)} = 7.118$, $p < 0.0019$] and a significant vagotomy × day interaction [$F_{interaction(6,45)} = 14.07$, $p < 0.0001$] compared to the vehicle group. Tukey post-hoc test showed that vagotomy prevented the increase in ethanol intake induced by the i.p. administration of bEVs derived from the gut microbiota of UChB-Alcohol rats, compared to rats that underwent sham surgery and received the same bEVs or those that underwent sham surgery and received the vehicle. Data are presented as mean ± SEM; $n = 6$ per experimental group. (C) Daily ethanol intake of two groups of Wistar rats without vagotomy that received UChB-Alcohol bEVs (7.9×10^8 bEVs) or vehicle via oral gavage for 3 consecutive days. A two-way analysis of variance (ANOVA) (treatment × day) revealed significant effect of the treatment [$F_{treatment(1,8)} = 22.00$, $p < 0.0016$], day [$F_{day(1946,15.57)} = 19.92$, $p < 0.0001$] and a significant treatment × day interaction [$F_{interaction(3,24)} = 19.21$, $p < 0.0001$] compared to the vehicle group. Sidak's post-hoc test indicated that the administration of UChB-Alcohol bEVs by oral gavage significantly increased voluntary ethanol intake in male Wistar rats, reaching the maximum difference between groups at Day 4 ($p < 0.05$). Data are presented as mean ± SEM; $n = 5$ per experimental group. (D) Daily ethanol intake of vagotomised or sham-operated Wistar rats, receiving UChB-Alcohol bEVs (7.9×10^8 bEVs) or vehicle via oral gavage for 3 consecutive days. Two-way analysis of variance (ANOVA) revealed significant effect of treatment [$F_{treatment(2,11)} = 17.27$, $p < 0.0001$], but not of day [$F_{day(1946,21.41)} = 1.882$, $p = 0.1774$ N.S.], compared to the vehicle group. Tukey post hoc test showed that vagotomy prevented the increase in ethanol intake induced by oral gavage administration of UChB-Alcohol bEVs, reaching the maximum difference at Day 4 compared to rats that underwent sham surgery and received the same bEV dose ($p < 0.05$) or those that underwent sham surgery and received the vehicle ($p < 0.05$). Data are presented as mean ± SEM; $n = 5$ per experimental group.

underscore the pivotal role of the vagus nerve in mediating the communication between the gut microbiota and the brain axis in the context of alcohol-related behaviours. This highlights the potential for interventions aimed at modulating alcohol consumption through the regulation of microbiota-gut-vagus nerve-brain communication pathways.

4 | Discussion

This study proposes gut microbiota-derived bEVs as a novel mechanism mediating gut microbiota-induced high alcohol intake. Our study revealed that gut microbiota-derived bEVs from a genetically selected high-alcohol-drinking rat strain (UChB rats) significantly increase voluntary alcohol consumption when administered to an alcohol-rejecting rat strain (Wistar rats). We isolated EVs enriched in bacterial vesicles (bEVs) from the gut microbiota of UChB rats, with or without a previous 120-day history of voluntary alcohol consumption. These bEVs administered to male and female Wistar rats via intraperitoneal injection and oral gavage significantly increased alcohol consumption, highlighting the robust influence of the gut microbiota inherent to UChB rats, also called innate microbiota.

While some prior studies required the use of germ-free mice or to modify the recipient microbiota using antibiotics or laxatives to observe behavioural effects, including ethanol intake (Wolstenholme et al. 2022; Wortelboer et al. 2023; Zhao et al. 2020), it is noteworthy that the UChB-derived bEVs did not require any pretreatment of the recipient Wistar rats to exert their pro-addictive effects. These results demonstrate that bEVs alone are sufficient to transmit alcohol-addictive behaviour between different rat strains without requiring bacterial colonisation in the recipient's gut. Furthermore, the induced behavioural effects on voluntary alcohol consumption are more pronounced in females than in males.

To better understand how the origin of the bEVs impacted drinking behaviour, we sequenced faecal samples from which the vesicles were isolated. 16S rRNA sequencing analysis revealed similar taxa richness within samples; however, β-diversity analysis showed that the three faecal sources segregated significantly distinguishable from each other. This suggests that drinking behaviour may not be attributable to the overall abundance of gut microbiota, but rather to specific gut microbiota compositions. At the genus level, *Phascolarctobacterium*—part of Bacillota C phylum—showed a higher relative abundance in both UChB groups compared to Wistar animals, suggesting that these bacteria might play a role in promoting drinking behaviour. Interestingly, Bacillota C phylum is part of the previously named *Firmicutes phylum*, which has been reported to be decreased in UChB rats with reduced drinking behaviour after antibiotic treatment (Ezquer et al. 2021). Additionally, Firmicutes have been found to have a significantly higher relative abundance in patients with alcoholic liver disease (ALD) (Chen et al. 2022).

Unlike conventional methods using bacterial monocultures (Zhao et al. 2020), in this study, bEVs were isolated directly from faeces to capture the full microbial diversity of the intestine, including non-culturable bacteria. The influence that each type of bEV has on the gut-brain axis remains to be elucidated since

this phenomenon is likely shaped by multiple factors, including the composition of the molecular cargo (lipids, proteins, nucleic acids, metabolites, among others), the lipoprotein profile on bEV's surface membranes, and the concentration of interacting particles within the axis (Fyfe et al. 2023; Liang et al. 2022; Thapa et al. 2023). This study confirmed the bacterial origin of the isolated bEVs through the identification of specific markers and molecular content. The isolation process, which included multiple purification steps such as filtration, ultracentrifugation and size exclusion chromatography, ensured the enrichment of bEVs while minimising potential contaminants. These vesicles displayed heterogeneous sizes and abundances, reflecting the taxonomic and functional diversity of the gut microbiota. NTA analysis revealed that bEVs from all experimental groups predominantly exhibited particle sizes in the 150–400 nm range, consistent with previously reported dimensions for bacterial vesicles (Northrop-Albrecht et al. 2022).

Molecular analysis demonstrated the presence of nucleic acids, including DNA and RNA, in all bEV samples, consistent with prior reports (Bitto, Zavan et al. 2021; Northrop-Albrecht et al. 2022). Normalisation of quantification by particle number revealed comparable nucleic acid levels across all groups. These findings emphasize the importance of normalising molecular content by vesicle number for accurate comparisons and highlight the potential of bEVs as carriers of genetic material involved in interbacterial communication or host modulation (Bitto, Cheng et al. 2021; Bitto, Zavan et al. 2021). TEM images confirmed the presence of vesicles exhibiting characteristics of bacterial EVs, displaying diverse EV's electron density profiles. These variations in density could reflect differences in vesicle composition, structural integrity, Gram categorisation of parental cells, and other factors dependent on the parental bacterial species and their specific metabolic state. LPS and OmpA, both Gram-negative bacterial markers (Tulkens et al. 2020), as well as LTA, a Gram-positive bacterial marker, were confirmed in all isolated bEV samples, corroborating their Gram-negative and Gram-positive origin. No signals for eukaryotic EV markers (Alix, Flotillin-1, and Syntenin-1) or eukaryotic non-EV markers (TOMM20 and Calnexin) were detected in this study, possibly due to their extremely outnumbered counts compared to microbial components present in the gut. However, it is important to note that the absence of universal markers for bEVs, along with the overlap in size and density with other submicron particles such as eukaryotic EVs or viral particles, hinders the isolation of pure bEV fractions. Although we confirmed the enrichment of bEVs by the above-mentioned bacterial markers, and the likely absence of eukaryotic EVs, the influence of donor-derived EVs or microbiota-derived viruses in the pool of isolated particles cannot be fully discarded. The limitations of current purification methods when working with complex microbial environments must be acknowledged. This becomes particularly relevant when the goal is to attribute a biological effect to a specific type or subpopulation of EVs. Techniques such as immunoaffinity-based separation or advanced density-gradient ultracentrifugation could improve purity.

To our knowledge, this study is the first to report the role of bEVs in promoting alcohol intake. Systemic and brain inflammation have previously been associated to the promotion of high alcohol intake (Blednov et al. 2011; Everitt and Robbins 2005; Koob and

Volkow 2016; Ostlund and Balleine 2005). Therefore, we expected to observe peripheral and brain inflammation in the Wistar animals injected with the UChB-derived bEVs. However, using a comprehensive battery of complementary techniques, we found no increase in pro-inflammatory markers in animals that received UChB-derived bEVs. This strongly suggests that systemic and brain inflammation are not required to induce the behavioural change that promotes alcohol-drinking behaviour in Wistar rats receiving UChB-derived bEVs. Subsequent analyses should explore additional neuronal pathways associated with addiction, such as alterations in neurotransmitters levels (dopamine and glutamate) or expand the analysis to other brain areas like the hippocampus or the nucleus of the solitary tract, where the sensory branches of the vagus nerve arrive to the brain (Koob and Volkow 2016). Additionally, a more detailed analysis of the bEVs composition found in our pooled particles might allow the identification of common bEV types in both UChB bEVs, which could be the critical component of increased drinking behaviour.

Our experiments aimed to unravel the naturally occurring mechanism through which gut microbiota drives alcohol consumption. This was our first study investigating gut microbiota-derived bEVs and their ability to promote high ethanol intake. Thus, we aimed to deliver the bEVs in close proximity to the vagus nerve as a first approach—choosing the intraperitoneal injection route—since the vagus nerve is reported to be the primary neural communication pathway between gut microbiota and the brain (Bravo et al. 2011; Cryan and Dinan 2012; Lee et al. 2020; Thapa et al. 2023). After observing the robust effect of the i.p.—delivered UChB-bEVs on drinking behaviour, we repeated the drinking assessment experiment using the same bEV dose but delivered via oral gavage, since this delivery route better simulates the natural location of bEVs. Surprisingly, animals that received bEVs via oral gavage consumed a similar amount of ethanol compared to those receiving bEVs via i.p. injection, albeit with different kinetics. By performing a vagotomy on the Wistar rats before bEVs administration—either i.p. or by oral gavage—we confirmed that administered bEVs also rely on the vagus nerve to exert their effects. For this purpose, all the injected animals received UChB-Alcohol bEVs, which may be closer in composition to the bEVs from microbiota of AUD patients. These results are consistent with previous reports showing that bEVs isolated from specific bacterial strains, which are increasingly detected in the faeces of elderly adults, induced cognitive impairment in a vagus nerve-dependent manner when orally administered to young mice (Lee et al. 2020). Therefore, our results suggest bEVs might trigger drinking behaviour by interacting with the vagus nerve, either directly (as shown in the i.p. experiments) or indirectly (as shown in the oral gavage experiments), possibly mediated by intestinal cells. It has been previously described that neuropods, enteroendocrine cells that physically interact with the vagus nerve, form a sort of synapse by releasing glutamate (Kaelberer et al. 2018). Whether bEVs stimulate the vagus nerve to signal to the brain or they can enter and directly traffic to the brain remains to be elucidated. Further investigation should address in more detail how and why vagotomy influences the microbiota-gut-brain-axis, since this procedure appears to be strain-specific (Bercik et al. 2011; Lee et al. 2020) and, because vagotomy can also alter the composition of gut microbiota, increasing Bacteroidetes and decreasing Proteobacteria and Verrucomicrobia in mice (Lee et al. 2020).

An important limitation of the present study is that we did not determine which specific cargo within the UChB-derived bEVs was responsible for inducing high alcohol intake in recipient animals. It is well known that bEVs are complex and heterogeneous structures composed of diverse biomolecules, including proteins, lipids, nucleic acids and toxins, among others. These molecules act synergistically and in a multifactorial manner, likely requiring their combined presence to trigger specific biological responses (Hosseini-Giv et al. 2022; Peregrino et al. 2024). This complexity makes it unlikely to attribute the observed effects to a single component. Identifying a single component or a small group of components would require extensive analyses, including detailed characterisation of proteins, lipids, nucleic acids, toxins, metabolites and the bEV corona, as well as functional studies to evaluate the impact of each component on alcohol-related behaviour. Further studies aimed at identifying these molecules and elucidating the specific mechanisms by which they induce high drinking behaviour are warranted, as they could pave the way for developing new therapeutic strategies to treat this devastating disease.

5 | Conclusion

In conclusion, this study proposes gut microbiota-derived extracellular vesicles as a novel mechanism mediating high alcohol intake in both male and female animals independent of inflammatory processes. Furthermore, we demonstrate that the isolated particles can transmit this reinforcing/addictive behaviour between different rat strains, in a vagus nerve-dependent manner.

Author Contributions

Macarena Díaz-Ubilla: conceptualization (equal), data curation (equal), formal analysis (equal), funding acquisition (equal), investigation (equal), methodology (equal), writing–original draft (equal), writing–review and editing (equal). **Aliosha I. Figueroa-Valdés**: data curation (equal), formal analysis (equal), writing–review and editing (equal). **Hugo E. Tobar**: data curation (equal), formal analysis (equal), methodology (equal), writing–review and editing (equal). **María Elena Quintanilla**: conceptualization (equal), data curation (equal), formal analysis (equal), investigation (equal), writing–review and editing (equal). **Eugenio Díaz**: data curation (equal), formal analysis (equal), writing–review and editing (equal). **Paola Morales**: data curation (equal), formal analysis (equal), writing–review and editing (equal). **Pablo Berríos-Cárcamo**: data curation (equal), formal analysis (equal), writing–review and editing (equal). **Daniela Santapau**: data curation (equal), formal analysis (equal), methodology (equal), writing–review and editing (equal). **Javiera Gallardo**: data curation (equal), formal analysis (equal), writing–review and editing (equal). **Cristian De Gregorio**: data curation (equal), formal analysis (equal), writing–review and editing (equal). **Juan Ugalde**: data curation (equal), formal analysis (equal), methodology (equal), writing–review and editing (supporting). **Carolina Rojas**: data curation (equal), formal analysis (equal), methodology (equal), writing–review and editing (equal). **Antonia Gonzalez-Madrid**: formal analysis (equal), investigation (equal), writing–review and editing (equal). **Marcelo Ezquer**: data curation (equal), formal analysis (equal), writing–review and editing (equal). **Yedy Israel**: conceptualization (equal), investigation (equal), writing–review and editing (equal). **Francisca Alcayaga-Miranda**: data curation (equal), formal analysis (equal), funding acquisition (equal), investigation (equal), writing–original draft (equal), writing–review and editing (equal). **Fernando Ezquer**: conceptualization (equal),

Data Availability Statement

Data supporting this study are included within the article and supporting material. The 16S rRNA sequencing data have been deposited in the Bioproject (NIH) database under the accession number PRJNA1195973, https://www.ncbi.nlm.nih.gov/bioproject/PRJNA1195973.

References

Agrawal, R. G., A. Hewetson, C. M. George, P. J. Syapin, and S. E. Bergeson. 2011. "Minocycline Reduces Ethanol Drinking." *Brain, Behavior, and Immunity* 25, no. 1: S165–169.

Alcohol DaABA. 2008. Global Status Report on Alcohol and Health. https://wwwwhoint/publications/i/item/9789241565639.

Bajaj, J. S., E. A. Gavis, A. Fagan, et al. 2021. "A Randomized Clinical Trial of Fecal Microbiota Transplant for Alcohol Use Disorder." *Hepatology* 73: 1688–1700.

Barnett, D. A., I. Arts, and J. Penders. 2021. "microViz: An R Package for Microbiome Data Visualization and Statistics." *Journal of Open Source Software* 6: 3201.

Bercik, P., E. Denou, J. Collins, et al. 2011. "The Intestinal Microbiota Affect Central Levels of Brain-Derived Neurotropic Factor and Behavior in Mice." *Gastroenterology* 141, no. 2: 599–609.e3.

Berent, D., and M. Wojnar. 2021. "Does Parental Alcohol Use Influence Children's Age at First Alcohol Intake? A Retrospective Study of Patients With Alcohol Dependence." *Healthcare* 9: 841.

Berleman, J., and M. Auer. 2013. "The Role of Bacterial Outer Membrane Vesicles for Intra- and Interspecies Delivery." *Environmental Microbiology* 15: 347–354.

Bitto, N. J., L. Cheng, E. L. Johnston, et al. 2021. "*Staphylococcus aureus* Membrane Vesicles Contain Immunostimulatory DNA, RNA and Peptidoglycan That Activate Innate Immune Receptors and Induce Autophagy." *Journal of Extracellular Vesicles* 10: e12080.

Bitto, N. J., L. Zavan, E. L. Johnston, T. P. Stinear, A. F. Hill, and M. Kaparakis-Liaskos. 2021. "Considerations for the Analysis of Bacterial Membrane Vesicles: Methods of Vesicle Production and Quantification Can Influence Biological and Experimental Outcomes." *Microbiology Spectrum* 9: e0127321.

Blednov, Y. A., J. M. Benavidez, C. Geil, S. Perra, H. Morikawa, and R. A. Harris. 2011. "Activation of Inflammatory Signaling by Lipopolysaccharide Produces a Prolonged Increase of Voluntary Alcohol Intake in Mice." *Brain, Behavior, and Immunity* 25, no. 1: S92–S105.

Bravo, J. A., P. Forsythe, M. V. Chew, et al. 2011. "Ingestion of Lactobacillus Strain Regulates Emotional Behavior and Central GABA Receptor Expression in a Mouse via the Vagus Nerve." *Proceedings of the National Academy of Sciences* 108: 16050–16055.

Callahan, B. J., P. J. McMurdie, M. J. Rosen, A. W. Han, A. J. Johnson, and S. P. Holmes. 2016. "DADA2: High-Resolution Sample Inference From Illumina Amplicon Data." *Nature Methods* 13: 581–583.

Castano, C., A. Novials, and M. Parrizas. 2023. "An Overview of Inter-Tissue and Inter-Kingdom Communication Mediated by Extracellular Vesicles in the Regulation of Mammalian Metabolism." *International Journal of Molecular Sciences* 24: 2071.

Chen, G., F. Shi, W. Yin, et al. 2022. "Gut Microbiota Dysbiosis: The Potential Mechanisms by Which Alcohol Disrupts Gut and Brain Functions." *Frontiers in Microbiology* 13: 916765.

Cryan, J. F., and T. G. Dinan. 2012. "Mind-Altering Microorganisms: The Impact of the Gut Microbiota on Brain and Behaviour." *Nature Reviews Neuroscience* 13: 701–712.

da Veiga Leprevost, F., B. A. Gruning, S. Alves Aflitos, et al. 2017. "BioContainers: An Open-Source and Community-Driven Framework for Software Standardization." *Bioinformatics* 33: 2580–2582.

Dhaher, R., K. K. McConnell, Z. A. Rodd, W. J. McBride, and R. L. Bell. 2012. "Daily Patterns of Ethanol Drinking in Adolescent and Adult, Male and Female, High Alcohol Drinking (HAD) Replicate Lines of Rats." *Pharmacology Biochemistry and Behavior* 102: 540–548.

Erickson, E. K., A. J. DaCosta, S. C. Mason, Y. A. Blednov, R. D. Mayfield, and R. A. Harris. 2021. "Cortical Astrocytes Regulate Ethanol Consumption and Intoxication in Mice." *Neuropsychopharmacology* 46: 500–508.

Everitt, B. J., and T. W. Robbins. 2005. "Neural Systems of Reinforcement for Drug Addiction: From Actions to Habits to Compulsion." *Nature Neuroscience* 8: 1481–1489.

Ezquer, F., M. E. Quintanilla, P. Morales, et al. 2022. "A Dual Treatment Blocks Alcohol Binge-Drinking Relapse: Microbiota as a New Player." *Drug and Alcohol Dependence* 236: 109466.

Ezquer, F., M. E. Quintanilla, F. Moya-Flores, et al. 2021. "Innate Gut Microbiota Predisposes to High Alcohol Consumption." *Addiction Biology* 26: e13018.

Ferretti, P., E. Pasolli, A. Tett, et al. 2018. "Mother-to-Infant Microbial Transmission From Different Body Sites Shapes the Developing Infant Gut Microbiome." *Cell Host & Microbe* 24: 133–145.e135.

Figueroa-Valdes, A. I., C. de la Fuente, Y. Hidalgo, et al. 2021. "A Chemically Defined, Xeno- and Blood-Free Culture Medium Sustains Increased Production of Small Extracellular Vesicles From Mesenchymal Stem Cells." *Frontiers in Bioengineering and Biotechnology* 9: 619930.

Frakes, A. E., L. Ferraiuolo, A. M. Haidet-Phillips, et al. 2014. "Microglia Induce Motor Neuron Death via the Classical NF-kappaB Pathway in Amyotrophic Lateral Sclerosis." *Neuron* 81: 1009–1023.

Fyfe, J., I. Casari, M. Manfredi, and M. Falasca. 2023. "Role of Lipid Signalling in Extracellular Vesicles-Mediated Cell-to-Cell Communication." *Cytokine & Growth Factor Reviews* 73: 20–26.

Gruning, B., R. Dale, A. Sjodin, et al. 2018. "Bioconda: Sustainable and Comprehensive Software Distribution for the Life Sciences." *Nature Methods* 15: 475–476.

Haas-Neill, S., and P. Forsythe. 2020. "A Budding Relationship: Bacterial Extracellular Vesicles in the Microbiota-Gut-Brain Axis." *International Journal of Molecular Sciences* 21, no. 23: 8899.

Hosseini-Giv, N., A. Basas, C. Hicks, E. El-Omar, F. El-Assaad, and E. Hosseini-Beheshti. 2022. "Bacterial Extracellular Vesicles and Their Novel Therapeutic Applications in Health and Cancer." *Frontiers in Cellular and Infection Microbiology* 12: 962216.

Hou, K., Z. X. Wu, X. Y. Chen, et al. 2022. "Microbiota in Health and Diseases." *Signal Transduction and Targeted Therapy* 7: 135.

Howland, R. H. 2014. "Vagus Nerve Stimulation." *Current Behavioral Neuroscience Reports* 1: 64–73.

Israel, Y., E. Karahanian, F. Ezquer, et al. 2017. "Acquisition, Maintenance and Relapse-Like Alcohol Drinking: Lessons From the UChB Rat Line." *Frontiers in Behavioral Neuroscience* 11: 57.

Jurga, A. M., M. Paleczna, and K. Z. Kuter. 2020. "Overview of General and Discriminating Markers of Differential Microglia Phenotypes." *Frontiers in Cellular Neuroscience* 14: 198.

Kaelberer, M. M., K. L. Buchanan, M. E. Klein, et al. 2018. "A Gut-Brain Neural Circuit for Nutrient Sensory Transduction." *Science* 361: eaat5236.

Kiraly, D. D., D. M. Walker, E. S. Calipari, et al. 2016. "Alterations of the Host Microbiome Affect Behavioral Responses to Cocaine." *Scientific Reports* 6: 35455.

Koob, G. F., and N. D. Volkow. 2016. "Neurobiology of Addiction: A Neurocircuitry Analysis." *Lancet Psychiatry* 3: 760–773.

Leclercq, S., P. de Timary, N. M. Delzenne, and P. Starkel. 2017. "The Link Between Inflammation, Bugs, the Intestine and the Brain in Alcohol Dependence." *Translational Psychiatry* 7: e1048.

Lee, K., H. E. Vuong, D. J. Nusbaum, E. Y. Hsiao, C. J. Evans, and A. M. W. Taylor. 2018. "The Gut Microbiota Mediates Reward and Sensory Responses Associated With Regimen-Selective Morphine Dependence." *Neuropsychopharmacology* 43: 2606–2614.

Lee, K. E., J. K. Kim, S. K. Han, et al. 2020. "The Extracellular Vesicle of Gut Microbial Paenalcaligenes Hominis Is a Risk Factor for Vagus Nerve-Mediated Cognitive Impairment." *Microbiome* 8: 107.

Liang, X., N. Dai, K. Sheng, et al. 2022. "Gut Bacterial Extracellular Vesicles: Important Players in Regulating Intestinal Microenvironment." *Gut Microbes* 14: 2134689.

Loi, B., G. Colombo, P. Maccioni, M. A. Carai, F. Franconi, and G. L. Gessa. 2014. "High Alcohol Intake in Female Sardinian Alcohol-Preferring Rats." *Alcohol* 48: 345–351.

Mayfield, J., L. Ferguson, and R. A. Harris. 2013. "Neuroimmune Signaling: A Key Component of Alcohol Abuse." *Current Opinion in Neurobiology* 23: 513–520.

McMurdie, P. J., and S. Holmes. 2013. "phyloseq: An R Package for Reproducible Interactive Analysis and Graphics of Microbiome Census Data." *PLoS ONE* 8: e61217.

Northrop-Albrecht, E. J., W. R. Taylor, B. Q. Huang, J. B. Kisiel, and F. Lucien. 2022. "Assessment of Extracellular Vesicle Isolation Methods From Human Stool Supernatant." *Journal of Extracellular Vesicles* 11: e12208.

Ostlund, S. B., and B. W. Balleine. 2005. "Lesions of Medial Prefrontal Cortex Disrupt the Acquisition but Not the Expression of Goal-Directed Learning." *Journal of Neuroscience* 25: 7763–7770.

Ou, Z., B. Situ, X. Huang, et al. 2023. "Single-Particle Analysis of Circulating Bacterial Extracellular Vesicles Reveals Their Biogenesis, Changes in Blood and Links to Intestinal Barrier." *Journal of Extracellular Vesicles* 12: e12395.

Palacios, E., L. Lobos-Gonzalez, S. Guerrero, et al. 2023. "Helicobacter pylori Outer Membrane Vesicles Induce Astrocyte Reactivity Through Nuclear Factor-Kappaappa B Activation and Cause Neuronal Damage In Vivo in a Murine Model." *Journal of Neuroinflammation* 20: 66.

Patil, I. 2021. "Visualizations With Statistical Details: The 'Ggstatsplot' Approach." *Journal of Open Source Software* 6, no. 61: 3167.

Peregrino, E. S., J. Castaneda-Casimiro, L. Vazquez-Flores, et al. 2024. "The Role of Bacterial Extracellular Vesicles in the Immune Response to Pathogens, and Therapeutic Opportunities." *International Journal of Molecular Sciences* 25: 6210.

Quintanilla, M. E., Y. Israel, A. Sapag, and L. Tampier. 2006. "The UChA and UChB Rat Lines: Metabolic and Genetic Differences Influencing Ethanol Intake." *Addiction Biology* 11: 310–323.

Reyes, R. E. N., A. J. Al Omran, D. L. Davies, and L. Asatryan. 2020. "Antibiotic-Induced Disruption of Commensal Microbiome Linked to Increases in Binge-Like Ethanol Consumption Behavior." *Brain Research* 1747: 147067.

Schaack, B., T. Hindre, N. Quansah, D. Hannani, C. Mercier, and D. Laurin. 2022. "Microbiota-Derived Extracellular Vesicles Detected in Human Blood From Healthy Donors." *International Journal of Molecular Sciences* 23: 13787.

Schloss, P. D., K. D. Iverson, J. F. Petrosino, and S. J. Schloss. 2014. "The Dynamics of a Family's Gut Microbiota Reveal Variations on a Theme." *Microbiome* 2: 25.

Schuh, C., J. Cuenca, F. Alcayaga-Miranda, and M. Khoury. 2019. "Exosomes on the Border of Species and Kingdom Intercommunication." *Translational Research* 210: 80–98.

Skrzypczak-Wiercioch, A., and K. Salat. 2022. "Lipopolysaccharide-Induced Model of Neuroinflammation: Mechanisms of Action, Research Application and Future Directions for Its Use." *Molecules (Basel, Switzerland)* 27: 5481.

Song, S. J., C. Lauber, E. K. Costello, et al. 2013. "Cohabiting Family Members Share Microbiota With One Another and With Their Dogs." *Elife* 2: e00458.

Straub, D., N. Blackwell, A. Langarica-Fuentes, A. Peltzer, S. Nahnsen, and S. Kleindienst. 2020. "Interpretations of Environmental Microbial Community Studies Are Biased by the Selected 16S rRNA (Gene) Amplicon Sequencing Pipeline." *Frontiers in Microbiology* 11: 550420.

Thapa, H. B., S. P. Ebenberger, and S. Schild. 2023. "The Two Faces of Bacterial Membrane Vesicles: Pathophysiological Roles and Therapeutic Opportunities." *Antibiotics (Basel)* 12: 1045.

Tian, M., Q. Li, T. Zheng, et al. 2023. "Maternal Microbe-Specific Modulation of the Offspring Microbiome and Development During Pregnancy and Lactation." *Gut Microbes* 15: 2206505.

Tran, T. D. B., C. Monroy Hernandez, H. Nguyen, et al. 2023. "The Microbial Community Dynamics of Cocaine Sensitization in Two Behaviorally Divergent Strains of Collaborative Cross Mice." *Genes, Brain, and Behavior* 22: e12845.

Tulkens, J., G. Vergauwen, J. Van Deun, et al. 2020. "Increased Levels of Systemic LPS-Positive Bacterial Extracellular Vesicles in Patients With Intestinal Barrier Dysfunction." *Gut* 69: 191–193.

Valles-Colomer, M., A. Blanco-Miguez, P. Manghi, et al. 2023. "The Person-to-Person Transmission Landscape of the Gut and Oral Microbiomes." *Nature* 614: 125–135.

Wei, S., W. Peng, Y. Mai, et al. 2020. "Outer Membrane Vesicles Enhance Tau Phosphorylation and Contribute to Cognitive Impairment." *Journal of Cellular Physiology* 235: 4843–4855.

Welsh, J. A., D. C. I. Goberdhan, L. O'Driscoll, et al. 2024. "Minimal Information for Studies of Extracellular Vesicles (MISEV2023): From Basic to Advanced Approaches." *Journal of Extracellular Vesicles* 13: e12404.

Wolstenholme, J. T., J. M. Saunders, M. Smith, et al. 2022. "Reduced Alcohol Preference and Intake After Fecal Transplant in Patients With Alcohol Use Disorder Is Transmissible to Germ-Free Mice." *Nature Communications* 13: 6198.

Wortelboer, K., P. A. de Jonge, T. P. M. Scheithauer, et al. 2023. "Phage-Microbe Dynamics After Sterile Faecal Filtrate Transplantation in Individuals With Metabolic Syndrome: A Double-Blind, Randomised, Placebo-Controlled Clinical Trial Assessing Efficacy and Safety." *Nature Communications* 14: 5600.

Xie, L., W. Rungratanawanich, Q. Yang, et al. 2023. "Therapeutic Strategies of Small Molecules in the Microbiota-Gut-Brain Axis for Alcohol Use Disorder." *Drug Discovery Today* 28: 103552.

Zhao, W., Y. Hu, C. Li, et al. 2020. "Transplantation of Fecal Microbiota From Patients With Alcoholism Induces Anxiety/Depression Behaviors and Decreases Brain mGluR1/PKC Epsilon Levels in Mouse." *Biofactors* 46: 38–54.

Supporting Information

Additional supporting information can be found online in the Supporting Information section.